Colour adaptation modifies the long-wave *versus* middle-wave cone weights and temporal phases in human luminance (but not red–green) mechanism

C. F. Stromeyer III*†‡, A. Chaparro*†, A. S. Tolias* and R. E. Kronauer*

*Division of Applied Sciences and †Department of Psychology, Harvard University, Cambridge, MA 02138, USA

1. The human luminance (LUM) mechanism detects rapid flicker and motion, responding to a linear sum of contrast signals, L' and M', from the long-wave (L) and middle-wave (M) cones. The red–green mechanism detects hue variations, responding to a linear difference of L' and M' contrast signals.

2. The two detection mechanisms were isolated to assess how chromatic adaptation affects summation of L' and M' signals in each mechanism. On coloured background (from blue to red), we measured, as a function of temporal frequency, both the relative temporal phase of the L' and M' signals producing optimal summation and the relative L' and M' contrast weights of the signals (at the optimal phase for summation).

3. Within the red–green mechanism at 6 Hz, the phase shift between the L' and M' signals was negligible on each coloured field, and the L' and M' contrast weights were *equal* and of opposite sign.

4. Relative phase shifts between the L' and M' signals in the LUM mechanism were markedly affected by adapting field colour. For stimuli of 1 cycle deg^{-1} and 9 Hz, the temporal phase shift was zero on a green–yellow field (~570 nm). On an orange field, the L' signal lagged M' by as much as 70 deg phase while on a green field M' lagged L' by as much as 70 deg. The asymmetric phase shift about yellow adaptation reveals a spectrally opponent process which controls the phase shift. The phase shift occurs at an early site, for colour adaptation of the other eye had no effect, and the phase shift measured monocularly was identical for flicker and motion, thus occurring before the motion signal is extracted (this requires an extra delay).

5. The L' *versus* M' phase shift in the LUM mechanism was generally greatest at intermediate temporal frequencies (4–12 Hz) and was small at high frequencies (20–25 Hz). The phase shift was greatest at low spatial frequencies and strongly reduced at high spatial frequencies (5 cycle deg^{-1}), indicating that the receptive field surround of neurones is important for the phase shift.

6. These temporal phase shifts were confirmed by measuring motion contrast thresholds for drifting L cone and M cone gratings summed in different spatial phases. Owing to the large phase shifts on green or orange fields, the L and M components were detected about equally well by the LUM mechanism (at 1 cycle deg^{-1} and 9 Hz) when summed spatially in phase or in antiphase. Antiphase summation is typically thought to produce an equiluminant red–green grating.

7. At low spatial frequency, the relative L' and M' contrast weights in the LUM mechanism (assessed at the optimal phase for summation) changed strongly with field colour and temporal frequency.

8. The phase shifts and changing contrast weights were modelled with phasic retinal ganglion cells, with chromatic adaptation strongly modifying the receptive field surround. The cells summate L' and M' in their centre, while the surround L' and M' signals are both antagonistic to the centre for ~570 nm yellow adaptation. Green or orange adaptation is assumed to modify the L and M surround inputs, causing them to be opponent with respect to each other, but with reversed polarity on the green *versus* orange field (to explain the chromatic reversal of the phase shift). Large changes in the relative L' and M' weights on green *versus* orange fields indicate the clear presence of the spectrally opponent surround even at 20 Hz. The spectrally opponent surround appears sluggish, with a long delay (~20 ms) relative to the centre.

‡To whom correspondence should be addressed at the Division of Applied Sciences, Harvard University, Cambridge, MA 02138, USA.

Two distinct visual detection mechanisms receiving predominantly long-wave (L) and middle-wave (M) cone inputs can be distinguished in humans: a luminance (LUM) mechanism and a red–green (RG) colour mechanism. Detection experiments show that the RG mechanism responds to an equally weighted difference of L and M cone contrast signals (L' and M') on various coloured background adapting fields (Chaparro, Stromeyer, Chen & Kronauer, 1995). Macaque red–green cells (Derrington, Krauskopf & Lennie, 1984; Lee, Martin & Valberg, 1989) of the parvocellular (PC) pathway reveal approximately equal and opposite L' and M' contrast weights when probed with large test stimuli. Lesions of the PC cells severely impair detection of red and green colour differences (Merigan, 1989; Schiller, Logothetis & Charles, 1990).

The LUM mechanism is best revealed using rapid flicker or motion. The LUM mechanism responds to a weighted sum of L' and M', but the relative *contrast* weights may vary considerably with adapting field colour (Eisner & MacLeod, 1981; Stromeyer, Cole & Kronauer, 1987). Lesions of the phasic, magnocellular (MC) pathway strongly elevate contrast thresholds for detecting rapid flicker or motion (Schiller *et al.* 1990; Merigan, Byrne & Maunsell, 1991).

We isolated the RG and LUM mechanisms to study how adapting field colour affects summation of L' and M' signals, measuring both the relative temporal phase of the L' and M' signals that produces optimal summation and the changing relative L' and M' weights accompanying the phase shifts. In both these respects, the RG mechanism appears unaffected by chromatic adaptation, whereas the LUM mechanism is markedly affected. This is suprising since the LUM mechanism is traditionally thought to be achromatic.

Previous flicker studies have shown that chromatic adaptation clearly affects the LUM mechanism. Swanson, Pokorny & Smith (1988) observed that, at intermediate temporal frequencies (6 Hz), orange adapting backgrounds induced a considerable phase lag of the L' signal relative to M'; the phase shift weakly reversed on green backgrounds. Measurements at higher frequencies (15 Hz) showed that coloured backgrounds also influence the relative L' and M' weights (Eisner & MacLeod, 1981; Stromeyer *et al.* 1987). Orange backgrounds selectively suppressed the L' contrast signal (more than Weberian cone-selective adaptation predicts) while green backgrounds selectively suppressed the M' contrast signal.

Recent physiological measurements (Smith, Lee, Pokorny, Martin & Valberg, 1992) indicate that the phase shift between the L' and M' signals in the LUM mechanism arises in the MC retinal ganglion cells. The measurements were only made on an orange adapting field. Virtually *every* cell had a strong relative L' signal lag at low and intermediate temporal frequencies that disappeared near 20 Hz. The authors argue that these retinal phase shifts explain the pychophysical luminance phase shifts observed by Swanson *et al.* (1988). The phase shifts between L' and M' signals are ascribed to properties of these cells, since the temporal responses of the L and M photoreceptors *per se* appear to be very similar (Smith *et al.* 1992).

METHODS

Stimuli and calibration

Vertical, red-plus-green heterochromatic, sine-wave gratings (3·5 deg diameter) were superposed on monochromatic backgrounds (4·2 deg) seen in Maxwellian view (Stromeyer, Kronauer, Ryu, Chaparro & Eskew, 1995). The wavelength of the background (8 nm half-bandwidth (HBW)) was set from 470 to 670 nm (blue to deep red). There was a small black fixation point in the centre of the field. Gratings were produced with a pair of optically superposed, spectrally filtered red and green Tektronix 608 cathode ray tube monitors operating at a 106 Hz frame rate. The phosphors decayed to one-tenth intensity in $< 1{\cdot}2$ ms. Patterns were generated digitally, and contrasts were controlled with 12-bit digital-to-analog converters, suitably attenuated for very low contrast. Stimuli were viewed monocularly through a 3 mm artificial pupil and achromatizing lens. To reduce ocular chromatic parallax shifts between the red and green patterns (especially at the higher spatial frequencies), the head was stabilized with a hard dental impression on a rigid x-y-z translator and the observer made initial fine adjustments of the patterns to align retinally the red and green stripes of square-wave gratings.

The spectral radiance of each stimulus component was calibrated at the eye-piece at 1 nm intervals with a radiometer and monochromator (2 nm HBW). The spectral radiance distributions were then weighted by the Smith & Pokorny (1975) cone spectral sensitivities to determine the L and M cone contrast of the gratings on the different coloured backgrounds. Each heterochromatic grating is represented by a vector in the L' and M' cone-contrast co-ordinates (Fig. 6). L cone contrast, $L' = \Delta L/L$, is the increment in L cone stimulation owing to the amplitude of the grating, ΔL, normalized by mean L field stimulation, L; M cone contrast, M', is similarly defined for M cones. Contrast is specified by vector length, VL, in the cone-contrast co-ordinates: $\mathrm{VL} = ((L')^2 + (M')^2)^{1/2}$. On each coloured field luminance gratings are represented by a 45–225 deg vector (equal L and M modulation with the same sign).

The field colour and intensity is specified for the central 3·5 deg grating region including its underlying adapting background. This colour is indicated by the wavelength of the field 'metameric' (or matched) for the L and M cones alone, based on the Smith & Pokorny (1975) cone sensitivities. Short-wave (S) cones are ignored for this specification since the results show that the S cones do not affect the phase shift.

Measuring the relative phase shift

We isolated the RG or LUM mechanism (as described later) and measured the phase shift between the L' and M' signals with a flicker discrimination or motion quadrature protocol (Lee & Stromeyer, 1989; Stromeyer, Eskew, Kronauer & Spillmann, 1991; Stromeyer *et al.* 1995). In each protocol, two vertical heterochromatic gratings of the same spatial frequency were superposed, both sinusoidally reversing in contrast (counterphase flickering) at the same rate. The gratings typically had different chromatic properties (described later).

In the flicker discrimination protocol each trial contained two temporal intervals separated by 100 ms. One flickering grating (the 'pedestal') had fixed properties and was presented in both temporal

intervals. The other flickering grating (the 'test') was added *spatially in phase* with the pedestal and had the *same* intensity in both intervals. The test temporal phase with respect to the pedestal was inverted between the two intervals (temporal phase θ was compared with $(\theta - 180)$ deg). When RG was being isolated, the observer chose the interval with the greater apparent red–green flicker. When LUM was being isolated the observer chose the interval with the greater luminance flicker or 'agitation'. Frequency-of-seeing curves were measured to assess that temporal phase, θ, which yields 50%-chance discrimination.

The motion quadrature protocol was only used with LUM. As shown in Fig. 1, the flickering pedestal and test (pattern 1 and 2, thin lines) always had a *fixed spatial offset of 90 deg phase* (quadrature spatial phase). On each trial, the pedestal and test were presented in a single interval and the observer judged whether motion was to the left or right. Figure 1 shows that a rightward drifting grating (thick line) can be produced by the sum of two *identical* counterphase flickering gratings (thin lines) offset in relative spatial and temporal phase by 90 deg (spatial–temporal quadrature). The thin lines show the spatial profiles of the two stationary flickering patterns at different instants in time, with the vertical arrows indicating the momentary direction of modulation. When the test pattern is of lower mean contrast than the pedestal, flicker with superposed rightward motion is seen.

If the two counterphase patterns in Fig. 1 are identical (with the same chromatic properties) and are flickered temporally *in phase*, then the two patterns will sum as a *single* counterphase grating with no net motion. However, if the two flickering patterns have different chromatic properties, the visual response to one pattern might lag the response to the other, producing motion to the left or right. The direction of motion reveals which pattern produces the lagging response. By advancing the relative temporal phase of that pattern, the responses to the two patterns can be brought back into temporal phase, thereby nulling the motion. We estimated the motion null from frequency-of-seeing curves for judgements of left *versus* right motion. On each trial the test was added to the pedestal at relative temporal phase θ or $(\theta - 180)$ deg, randomly chosen to produce motion to left or right. The null is specified by the value of θ yielding chance performance. The procedure is efficient, for with a judicious initial choice of θ, the frequency-of-seeing curve can be measured in ~10 min.

On each presentation the temporal contrast envelopes of pedestal and test were ramped on together for 94 ms with a raised cosine, held constant for 470 ms, then ramped off with the cosine. (The duration was doubled for 1 Hz stimuli.) Tones signalled the trial intervals and gave response feedback. To assess the L' and M' contrast weights, a staircase procedure estimated contrast thresholds at the 71%-correct level. The pedestal contrast was fixed supra-threshold, and the test contrast was stepped down 0·1 log unit after two successive correct responses and stepped up the same amount after each error. Each threshold was based on the mean staircase reversals for several runs. Standard errors of the mean for the weight estimates were directly determined from these reversals.

Unique L cone and M cone stimuli for each observer

As explained later, phase measurements were made with an L test and an M test that uniquely stimulates the L and M cones. We calculated red and green light mixtures that produce these unique stimuli based on the Smith & Pokorny (1975) cone sensitivities; a psychophysical procedure was then used to make small corrections for each observer. These small corrections considerably improved consistency between the observers' results, especially for conditions in which LUM is considerably more sensitive to L' than to M'; for these conditions we wanted a good estimate of the unique M stimulus so that the more sensitive L signal did not intrude. This low *relative* M' sensitivity obtains for three conditions in particular: for the L' *versus* M' phase shift at 10–20 Hz on green fields and for

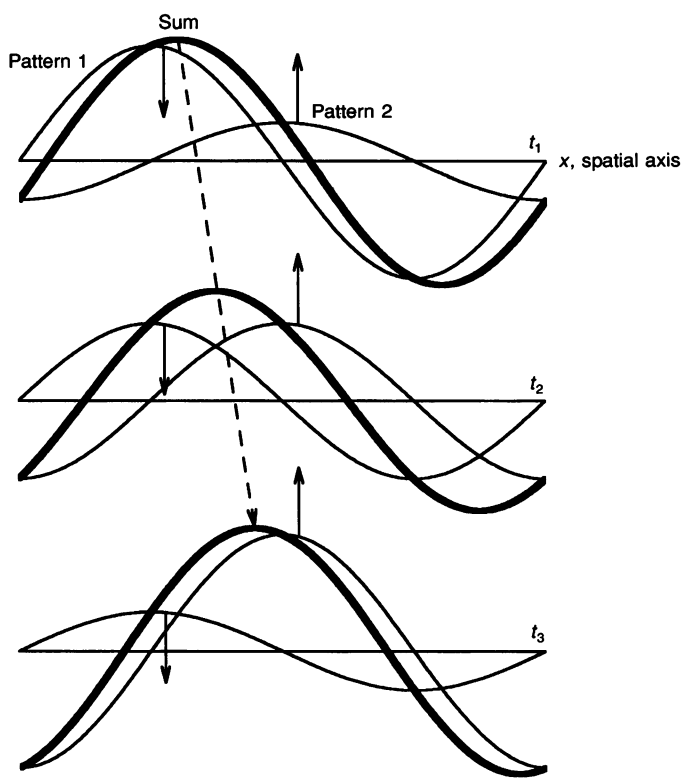

Figure 1. Quadrature motion protocol

The thick line shows the spatial profile of a rightward moving grating at equal time intervals (t). This grating can be produced by the sum of two identical stationary, contrast-reversing (counterphase) gratings (thin lines) offset in spatial and temporal phase by 90 deg (in spatial–temporal quadrature). In the quadrature motion protocol the 'test' (Pattern 2) is added to a constant 'pedestal' (Pattern 1) with a fixed spatial phase offset of 90 deg, and the relative temporal phase, θ, of the test is varied. Motion is reversed by inverting the temporal test phase (θ *versus* $(\theta - 180)$ deg), and direction discrimination is measured as a function of the test phase or contrast. The pedestal and test generally have different chromatic properties.

the estimates of the L' *versus* M' contrast weights at low temporal frequencies on orange fields and at 10–20 Hz on green fields.

We modified the cone isolation procedure of Stockman, MacLeod & Vivien (1993). They showed that L cones are strongly suppressed in detecting rapid flicker on a bright red field immediately after viewing a bright blue field. Conversely, the M cones are suppressed in detecting the flicker on a blue field just following a red field. Our preadapting field (blue 480 nm or red 661 nm) was presented for 3 s and then shifted to the other colour for 0·5 s. A pair of 1 cycle deg^{-1} and 9 Hz counterphase gratings, in spatial–temporal quadrature, were added to the latter field for the first 230 ms. This sequence was repeated continuously. To find the unique L direction, the gratings were presented on the red field which suppresses L cones. The pedestal grating was of maximal available contrast (red and green lights flickering in phase), and the adapting fields were as bright as possible for the task (1400–5000 troland (td)). The test grating was varied about the nominal L cone axis to find the red–green mixture producing a motion null (50% point on the frequency-of-seeing curve). The null ought to lie on the L axis, for here the M cone test contrast is zero and the L cones are presumably suppressed. The estimated L cone axis for observers A.C., A.S.T. and C.F.S. lay at −4, −5 and −2 deg, respectively, in the original L', M' cone-contrast co-ordinates based on Smith & Pokorny (1975) cone sensitivities. A similar experiment estimated the M cone axis for observers A.C., A.S.T. and C.F.S. to be 85, 85 and 91 deg, respectively.

The unique L and M cone stimuli of each observer were used for subsequent measurements. Threshold detection contours in the L', M' co-ordinates and estimates of the relative L' and M' contrast weights were corrected for each observer.

The observers were male from 25 to 53 years old who had normal colour vision (Farnsworth-Munsell 100-hue test). They participated with written informed consent. The study was approved by the university ethics committee and conformed to the Declaration of Helsinki.

Isolation of the LUM mechanism?

We use a quadrature motion protocol to isolate the LUM mechanism over a broad range of spatial and temporal frequencies. The protocol is a variation of the minimum motion technique of Anstis & Cavanagh (1983). In reviewing the LUM mechanism, Lennie, Pokorny & Smith (1993) stated that the MC pathway underlies the flicker photometrically measured luminosity function and perhaps that measured by minimum motion, and that the spectral sensitivity of retinal MC cells closely agrees with the human photopic luminosity function, V_λ. Isolation of the MC pathway may be promoted by our use of very low test contrast in the motion quadrature protocol; threshold test contrast is often as low as 0·05%. The protocol isolates an *opponent* motion mechanism, a mechanism highly sensitive to the *difference* of contrast of *opposite* motions (Stromeyer, Kronauer, Madsen & Klein, 1984). The flickering pedestal in the quadrature protocol strongly *facilitates* motion. By enhancing motion, the protocol may isolate the MC pathway over a broad range of spatial and temporal frequencies.

RESULTS

RG mechanism: L' *versus* M' phase shift and relative contrast weights

For RG, adapting fields of different colours do not appear to induce either a phase shift between the L' and M' signals or a change in the relative contrast weights. Measurements were made at 6 Hz, where colour sensitivity is still quite high. The lack of phase shift suggests that RG is isolated, for the LUM mechanism shows very large phase shifts at 6 Hz.

We measured the relative phase shift of the L' and M' signals with the flicker discrimination protocol, using gratings of 1 cycle deg^{-1} and 6 Hz on 2300 td adapting

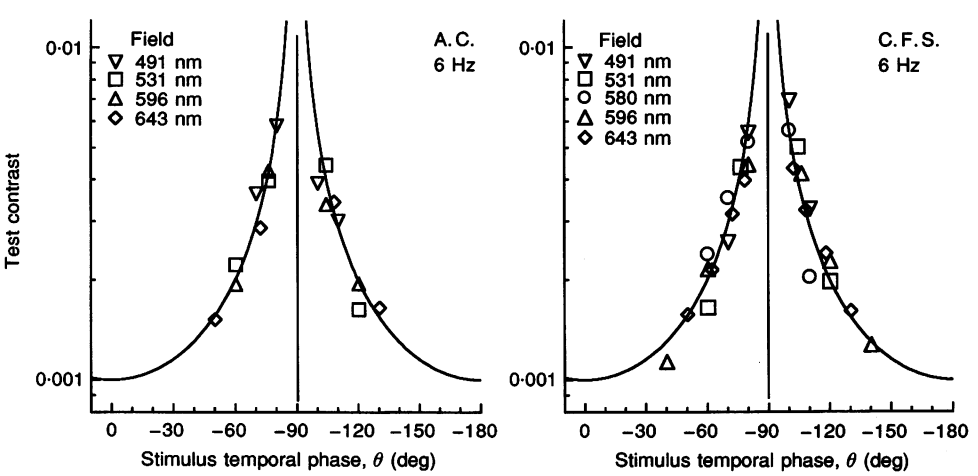

Figure 2. Phase shift between L' and M' signals in RG mechanism

Phase shift for two observers (A.C. and C.F.S.) measured at 6 Hz with patterns of 1 cycle deg^{-1} on coloured adapting fields from green to red. The L pedestal and M test were presented in the flicker discrimination protocol; the observer attempted to choose the test interval with greater red–green flicker. The M test contrast thresholds are shown as a function of relative temporal phase, θ, of pedestal and test. The template with symmetry axis at $\theta = -90$ deg shows the prediction for *no* intrinsic, physiological phase shift between the L' and M' signals; the phase shift in RG is very small as shown by the fit. Each data set is vertically scaled by a constant to fit the template (i.e. contrast normalized).

fields of blue (491 nm), green (531 nm), yellow (580 nm), orange (596 nm) and deep red (643 nm, 1300 td). The pedestal was an L cone counterphase pattern at twice contrast threshold so its red–green flicker was just apparent. The test was an M cone counterphase pattern added spatially in phase with the pedestal, with relative temporal phase θ deg *versus* $(\theta - 180)$ deg in the two temporal intervals of each trial. Figure 2 shows M test contrast thresholds, for discriminating the interval with the stronger red–green flicker, as a function of relative temporal phase, θ, of pedestal and test. If there was no intrinsic phase shift between the L' and M' signals in RG, discrimination should be best at $\theta = 0$ and -180 deg (and worst at $\theta = -90$ deg), with the thresholds conforming to the inverse cosine template, $|\cos\theta|^{-1}$ (Lee & Stromeyer, 1989). The results fitted this template. At the template peak the test and pedestal are combined in quadrature temporal phases and discrimination is poor. At the template trough sensitivity is maximal; in one trial interval the L' and M' stimuli are in temporal antiphase producing a maximal RG response, and in the other interval the stimuli are in temporal phase and thus cancel in RG. Results for each coloured field were fitted to the template by a single vertical shift of the data. In the worst case the fit could be improved by a 3 deg horizontal translation, indicating that the intrinsic phase shift between the L' and M' signals in RG at 6 Hz was 3 deg or less. The lack of phase shift on the deep-red field was also confirmed at 10 Hz.

The flicker discrimination protocol was used to compare the *relative* L' and M' weights on the green and orange fields at 2 and 6 Hz (observer C.F.S.). We have observed previously (Chaparro *et al.* 1995) that the RG detection contour for 200 ms flashes has a slope of ~1·0 in the L', M' cone-contrast co-ordinates on various coloured adapting fields. Presumably the coloured adapting field causes the cones to selectively adapt so that L and M *contrast* contributes equally to RG on each coloured field.

The present measurements show that the contrast weights are equal at 6 Hz on various coloured fields. The pedestal was set to 135–315 deg in the L', M' co-ordinates, at ~2 times threshold. Contrast thresholds were then separately measured for the L test and M test added to the pedestal in optimal phase. The thresholds specify the ratio of L' and M' weights in RG. The weight ratio was close to one: 0·92 and 1·0 on the green field and 0·99 and 0·97 on the orange field at 2 and 6 Hz, respectively. Note that it is the *ratio* of L' and M' weights that remains *constant* on the green and orange fields. The individual L' and M' weights were smaller on the orange field than the green fields, owing to adaptation at the opponent 'second-site' in the RG pathway (Chaparro *et al.* 1995).

Thus for the RG mechanism, chromatic adaptation has virtually no effect on the relative phase and relative contrast weights of the L' and M' signals. As argued later, properties of red–green PC cells might explain these results. These null results support the view that the large effects of chromatic adaptation observed in the remaining measurements reflect a different mechanism.

L' versus M' phase shift in LUM

The phase shifts in LUM were largely measured with the quadrature motion protocol, for it is easier to judge left *versus* right motion in a single interval than to judge the flicker strength across two intervals; it is especially easier at low temporal frequencies. However, limited measurements show that the phase shifts are identical for flicker and motion.

Measuring the phase shift with motion. Previously (Lee & Stromeyer, 1989; Stromeyer *et al.* 1995), we fitted phase templates to the quadrature motion data. The data show the test contrast required for discriminating the motion direction as a function of relative temporal phase, θ, of pedestal and test. The template has an inverse sine form $|\sin(\theta - \theta_0)|^{-1}$, where θ_0 is the stimulus phase for the motion null. The vertical symmetry axis (peak) of the template specifies θ for the motion null. When there is no intrinsic phase shift between the L' and M' signals, the template peaks at $\theta_0 = 0$ deg (pedestal and test temporally in phase).

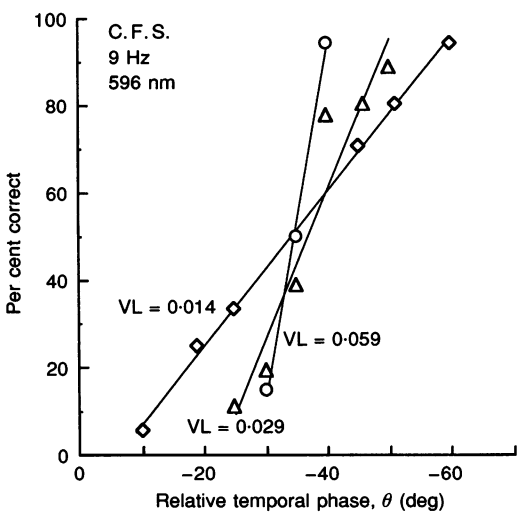

Figure 3. Frequency-of-seeing curves for left *versus* right motion discrimination in LUM mechanism

Measured with quadrature motion protocol with patterns of 9 Hz and 1 cycle deg^{-1} on an orange field (596 nm, 1300 td). The M test was combined in spatial quadrature with the fixed luminance pedestal; each curve is for a different contrast of the test (specified by vector length, VL, in the L', M' cone-contrast co-ordinates). At the motion null (50 % point on curve) the M test stimulus is delayed ~35 deg in temporal phase ($\theta = -35$ deg) relative to the luminance pedestal; hence, on the orange field, the M' signal is advanced ~35 deg relative to the luminance pedestal signal. Higher test contrast steepens the slope and improves sensitivity but has little influence on the null.

Measuring the template is time consuming, but the same phase information can be obtained from a frequency-of-seeing curve for left *versus* right motion judgements for several θ values just either side of the symmetry axis (presumed null). Measurements in Fig. 3 illustrate this abbreviated procedure.

To produce perceived motion the counterphase pedestal and test must both stimulate a *common* mechanism, since a single counterphase pattern has no net motion. The pedestal on each coloured background was adjusted to produce low contrast *luminance* flicker. This luminance pedestal is represented by a vector of 45–225 deg in the L', M' co-ordinates, lying *parallel* to the RG detection contour of slope 1·0, thus not stimulating RG. The phase shift between the L' and M' signals *generated by the luminance pedestal* provides a measure of the relative L' and M' phase shift in LUM. This was assessed using two separate test probes, combined in spatial quadrature phase with the luminance pedestal. First an L test was paired with the luminance pedestal, and the temporal phase of the test was varied to find the motion null. The null was then remeasured for an M test paired with the same pedestal. The phase shift between the L' and M' signals is given by the difference of the stimulus temporal phase shifts needed to achieve nulls with the L test and M test (Stromeyer *et al.* 1995).

The frequency-of-seeing curves (Fig. 3) show data using this abbreviated method, where the M test in this example is paired with the luminance pedestal. Measurements were made with gratings of 1 cycle deg^{-1} and 9 Hz on an orange field (596 nm, 1300 td), which induces a large phase shift (Fig. 4). Each curve is for a different contrast value of the M test, paired with a luminance pedestal of fixed contrast (VL = 0·064, pedestal vector length in L', M' co-ordinates). The motion null (at the 50%-chance point) is little affected by the test contrast, for the null lies at about $\theta = -35$ deg independent of test contrast. The null indicates that the M test signal leads the pedestal signal by ~35 deg. (In the full experiment we would also measure a curve for the L test; on the orange field the null would lie at a positive θ value.) The null corresponds to the symmetry axis of the template. Based on the shape of the template near the symmetry axis, the slope of the frequency-of-seeing data should vary approximately *linearly* with test contrast over this small range of θ, which is the case. The steeper slope at higher test contrast shows that one can make accurate motion judgements at θ values nearer the symmetry axis. For the remaining measurements, the pedestal and test were typically set to ~3 times threshold to produce precise phase estimates. The *effective* luminance contrast of the test at ~5 deg phase from the null is often as low as 1/10–1/20% contrast.

The retinal MC cells show a phase advance as contrast is raised, owing to an active *contrast gain* control (Benardete, Kaplan & Knight, 1992). The present measurements do not reflect this, either because the range of contrast is too low (Lee, Pokorny, Smith & Kremers, 1994) or the response to the pedestal and test both undergo an equivalent phase advance so the *relative* phase shift is constant.

Adapting field colour and the LUM phase shift. On each coloured field we assessed the L' *versus* M' signal phase shift

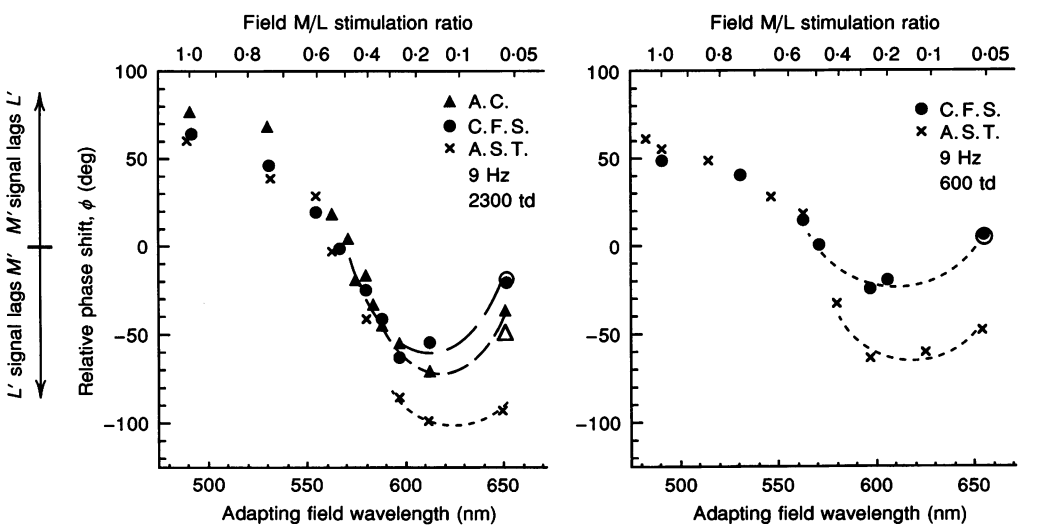

Figure 4. Phase shift, ϕ, between L' and M' signals in LUM on different coloured fields

Phase shift measured with quadrature motion protocol with patterns of 9 Hz and 1 cycle deg^{-1} on bright (2300 td) and moderate (600 td) fields. The phase shift is greatest on green (500 nm) and orange (600 nm) fields and crosses through zero on a green–yellow field of ~570 nm. Field colour is specified for the L and M cones alone; the top axis specifies the M/L field stimulation ratio and the bottom axis specifies field wavelength corresponding to this ratio. The sign of the phase shift is an arbitrary convention. ○ and △, phase shift measured 6–9 min following a full rod bleach produced with light of 520 nm and 7·3 log scotopic troland second for observers C.F.S. and A.C., respectively (see text).

from motion nulls for the L test and the M test paired with the luminance pedestal. Figure 4 shows the phase shifts for three observers measured with 1 cycle deg^{-1}, 9 Hz gratings on bright (2300 td) and moderate (600 td) fields. Field colour is specified by mean M/L cone stimulation (top axis) and the corresponding metameric (matching) wavelength (bottom axis), based on the Smith & Pokorny (1975) L and M cone spectral sensitivities. The phase shift was remarkably sensitive to field colour. The phase shift was zero on a green–yellow field of ~570 nm. On the brighter (2300 td) fields, the phase shift initially grew ~2·2 deg for each 1 nm change of the field away from 570 nm, but in opposite directions to either side of 570 nm. The curve thus resembles a chromatic opponent curve, suggesting that a spectrally opponent process within LUM controls the phase shift. On short-wave fields (490 nm) the M signal lags L by up to 70 deg and on orange fields (600 nm) the L signal lags M by up to 60 deg. This is contrary to the prediction of a simple latency difference of the cone photoreceptor responses *per se*. On orange fields the L cones are more light-adapted than M cones and thus might be expected to be faster, but the phase shift is in the opposite direction (Swanson *et al.* 1988).

The phase shift for two observers was smaller on the deep-red (650 nm) field than the orange field. The red field should light-adapt the L cones *considerably more* than the M cones and produce a small differential speeding up of the L cone response that may partially counteract the relative L signal lag otherwise seen on long-wave fields. (If this cone latency effect is to explain the red field results, we are puzzled by the lack of phase shift in RG on the red field.) The reduced LUM phase shift cannot be ascribed to an intruding rod signal, for the phase shift is little changed (Fig. 4, ○, △) when measured 6–9 min following a full rod bleach produced with light of 520 nm and 7·3 log scotopic troland second (Rushton & Powell, 1972). All observers remarked that, with adapting fields at the spectral extremes, the phase shifts reached an asymptotic value only after 2 min of adaptation. On the red field the phase shift decreased ~10 deg between 1 and 2 min adaptation, while on the blue field the phase shift grew a similar amount.

The field colour in Fig. 4 is specified by the M/L field ratio. That the S cones play little role was shown by varying mean S cone stimulation. We added uniform violet light of 421 nm and 10^{10} quanta deg^{-2} s^{-1} (195 td) to the 2300 td adapting fields, which strongly stimulates S cones while only slightly affecting L and M cones. The violet light added to a 522 nm green field caused the phase shift to decrease by 3 deg (observer C.F.S.), a shift consistent with a direct influence of the violet light on the L and M cones. The violet light shifts the effective or 'metameric' wavelength for these cones to a slightly longer wavelength (523 nm) by increasing mean L stimulation more than M. Adding the same violet light to a 566 nm green–yellow field caused the phase to change 3 deg in the opposite direction. The violet light now shifts the effective field wavelength in the opposite direction to a shorter wavelength (564 nm). The weak effect of the violet light can thus be explained by a small direct variation in the M/L field ratio and no S cone effect need be considered.

The phase shift occurs at a site more proximal than the cones, demonstrated by the fact that the *L′ versus M′* phase shift is negligible in RG but is large here. Further evidence that the large phase shifts are specific to LUM is that the phase shifts are still strongly present when the 9 Hz patterns are presented briefly. For 38 ms presentations, the *M′* signal lagged *L′* by 68 deg phase (observer C.F.S.) on the green field (503 nm, 1300 td) and *L′* lagged *M′* by 79 deg on the orange field (596 nm, 1300 td). Brief presentations strongly reduce the motion sensitivity of chromatic mechanisms compared with LUM mechanisms (Cropper & Derrington, 1994).

The phase shifts (Fig. 4) were greatest on green (~500 nm) and orange (~600 nm) fields, so these fields were used in the remaining measurements.

Monocular site for LUM phase shift. If the phase shift occurs at an early retinal or lateral geniculate nucleus (LGN) site, then changing the colour appearance of the field by adding uniform light to the non-test eye should have no effect. Phase measurements (observer C.F.S.) were made at 9 Hz with the gratings on the green–yellow (567 nm, 1300 td) field presented to the left eye, as before; this field produces zero relative phase shift. A circular adapting field of red or blue light of 2000 td was presented to the other eye and fused with the green–yellow field. The fused field appeared strongly orange or bluish, respectively. This altered colour had no effect on the phase shift.

The relative phase shift and summation of moving gratings in LUM. For a uniformly drifting sinusoidal grating, a spatial or temporal phase shift of the same magnitude (in deg phase) produces an identical stimulus change. The *temporal* phase shifts measured above should predict the requisite spatial phase shift for optimal summation of drifting L and M gratings.

This has important implications for studies on colour and motion. If the phase shift arises in the retina then nominally 'equiluminant' moving patterns may produce clear signals at higher stages in LUM. An equiluminant grating of red and green stripes is an L grating summed in spatial antiphase with an M grating of identical luminance contrast, thus producing no luminance variation across the surface of the grating (when stationary). When the pattern moves, there may be an appreciable lag between the *L′* and *M′* signals; this will bring the neural representations of the two antiphase gratings partially into spatial phase and create an effective luminance 'ripple'. The present results demonstrate that LUM can detect nominally equiluminant drifting gratings on the green or orange field (1300 td).

Contrast thresholds were measured for identifying whether the gratings moved left or right at 9 Hz. Thresholds were first measured for the separate L and M gratings to equate

their 'luminance' contrast. The two equated gratings were then summed in different spatial phases and the direction thresholds remeasured. Figure 5 shows how the two components summated as a function of their relative spatial phase. Each threshold point is based on four to six staircases. The summed threshold is expressed by the equation:

$$\text{Summed threshold} = (C_L/T_L) + (C_M/T_M),$$

where T_L and T_M are the threshold contrasts of the individual L and M components, and C_L and C_M are the contrasts of the components in the combined patterns. The L and M components were combined in *equal* threshold amounts. A value of 1·0 represents complete summation at the optimal relative phase, and higher values represent proportionally *less* summation. The curves show how the summed threshold is expected to vary for the two components linearly summating in LUM:

$$\text{Summed threshold} \propto \cos[(\theta - \phi_{LUM})/2]^{-1},$$

where θ is the relative spatial phase of the two stimulus components, and ϕ_{LUM} is the intrinsic phase shift between the L' and M' signals in LUM. The curve represents the reciprocal of the amplitude of the sum of two equally effective luminance spatial sinusoids (L and M, respectively) as a function of relative spatial phase. Lindsey, Pokorny & Smith (1986) used a similar curve to represent the effective luminance amplitude of a pair of red and green flickering lights summed in different temporal phases. The present results fit the template except near the peaks where another detection mechanism may intrude (Lindsey *et al.* 1986).

The troughs of the curves show approximately complete summation between the two components and the peaks show cancellation. The arrows in the troughs and near the peaks indicate, respectively, the phase for best summation and best cancellation estimated from the quadrature motion protocol. The relative phase shifts from the two methods agree reasonably well, but the quadrature protocol provides more precise estimates and is far more efficient (requiring several minutes rather than the several days for the present measurements).

On the green field (○), to achieve best summation the drifting M grating must be spatially advanced 70–80 deg in phase relative to the L grating to compensate for the relative M' signal lag, whereas on the orange field (△) the L pattern must be advanced ~60 deg. The motion is detected about equally well whether the L and M components are summed spatially in phase or in antiphase, i.e. at $\theta = 0$ or 180 deg. Thus owing to the large phase shifts, *luminance* motion is generated about equally well by the luminance and nominal chromatic patterns.

To confirm that LUM is isolated, we remeasured the summed threshold on the green field (observer C.F.S.) with

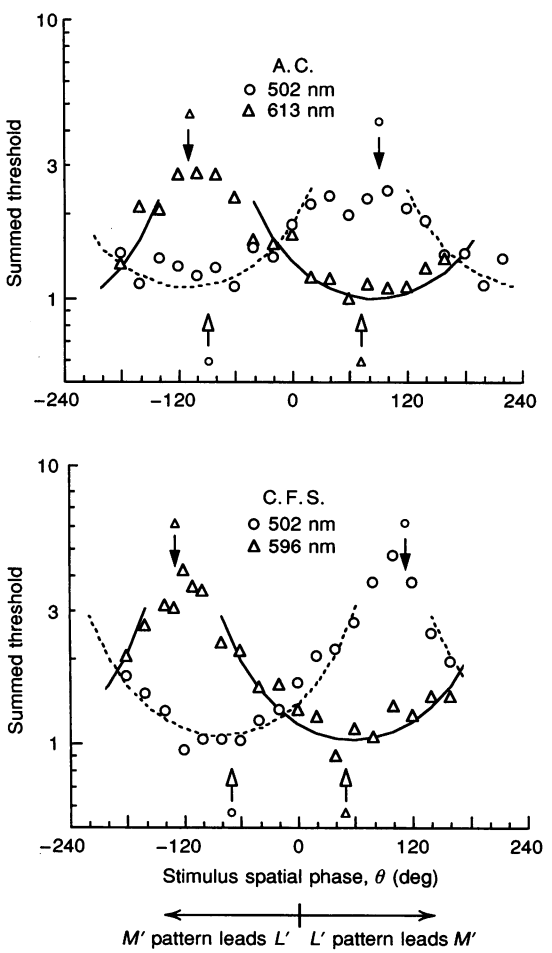

Figure 5. Motion direction discrimination thresholds for a drifting L grating and M grating summed in different relative spatial phases, θ, on green and orange fields

The two gratings of 1 cycle deg^{-1} drifted left or right together at 9 Hz. The two components were first equated in effective contrast for the direction discrimination task. A summed threshold of 1·0 represents complete visual summation of the L and M patterns at the optimal phase, i.e. each component in the combined pattern has one-half the contrast measured individually. The average S.E.M. of the data points is 14 and 13% for observers A.C. and C.F.S., respectively, with a maximal value of 21 and 20%, respectively. Higher values indicate proportionately higher contrast thresholds. For optimal summation (at bottom of trough) on the green field (○), the M pattern is spatially advanced by ~70 deg phase relative to the L pattern; on the orange field (△), the L pattern is ~60 deg advanced. Arrows show estimated phase for best and worst summation from the quadrature motion protocol. Fitted curves show the linear prediction of summation in LUM (see text).

brief 38 ms presentations of the 9 Hz drifting gratings; this penalizes chromatic motion detection (Cropper & Derrington, 1994). The L and M gratings summed equally well whether combined spatially in phase or antiphase (with less than 3% threshold difference).

A more convincing way of showing that LUM is isolated is to measure complete threshold contours in the L', M' cone-contrast co-ordinates for identifying the direction of motion. The 9 Hz drifting L and M components were combined in various amplitude ratios (both positive and negative) on the green field. Figure 6 (□) shows thresholds for the case where the drifting M component is advanced 80 deg in spatial phase relative to the L component to compensate for the M' signal lag. The *straight* detection contours of negative slope indicate that the L' and M' signals positively summate at optimal phase in LUM. The contour is represented by:

$$|aL' + bM'| = \text{constant},$$

with a and b specifying the L' and M' contrast weights for LUM.

The ellipse (Fig. 6, ○) represents similar measurements where we did not compensate for the intrinsic phase shift; the drifting L and M components were combined spatially in phase in quadrants 1 and 3 and in spatial antiphase in quadrants 2 and 4. The ellipse was fitted using the parameters $a/b = 2{\cdot}2$ (specifying the relative L' and M' weights) and $\phi = 80$ deg (specifying the intrinsic M' signal lag). An elliptical detection contour alone cannot provide information about the chromatic properties of visual mechanisms (Poirson, Wandell, Varner & Brainard, 1990). However, the good simultaneous fit of the ellipse *and* straight contours with the same two parameters demonstrates that the motion is detected by a single luminance mechanism which linearly sums L' and M'. LUM thus detects all the moving gratings that lie on the ellipse (Fig. 6), including the nominally equiluminant grating on an axis parallel to the straight detection contours.

How can a *temporal* phase shift, possibly arising in retinal MC cells, lead to a *spatial* phase shift between the drifting L and M components? The spatial phase shift results from the fact that the *stimulus itself* is drifting uniformly in one direction. The spatially distributed array of MC cells may simply act to *temporally* advance or retard the effective instantaneous spatial contrast profile, independently for the L and M patterns.

Effect of spatial frequency on the LUM phase shift. We next measured the influence of spatial and temporal frequency on the phase shift, using the quadrature motion protocol. These parameters are important for modelling the effects. Spatial frequency is considered first. The adapting field was set to 1300 td so that there would be sufficient contrast; this field level was typically used for the remaining measurements.

Figure 7 shows the phase shift measured at 9 Hz. The phase shift was approximately zero at all spatial frequencies on the green–yellow field (571 nm), measured for observer A.S.T. On the green (504 nm) and orange (596 nm) fields the phase shift was greatest at low spatial frequency and decreased considerably as spatial frequency was raised to 4–5 cycle deg^{-1}. However, even at these higher spatial frequencies the phase shift was still clearly present on the green field. Measurements were not extended to higher spatial frequencies owing to the difficulty of retinally aligning the two flickering chromatic patterns so that there would be no motion bias to left or right.

The large phase shifts at *low* spatial frequencies suggest that the receptive field surround is important for the phase shift. Smith *et al.* (1992) observed large relative phase shifts between L' and M' signals in MC ganglion cells with large stimuli which stimulated both centre and surround; the phase shifts vanished with a small, centre-isolating stimulus. This was confirmed by Kremers, Yeh & Lee (1994).

The centre response can be isolated with sufficiently fine gratings, for the small centre may 'see' a good fraction of a single bar and thus respond well, but the larger surround may integrate over a number of light–dark spatial cycles

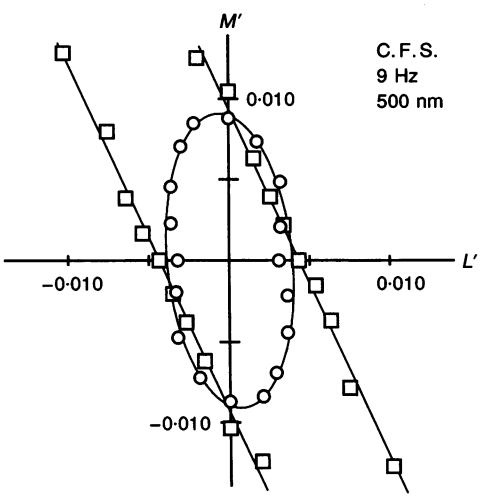

Figure 6. Thresholds in L', M' cone-contrast co-ordinates for direction discrimination of drifting 9 Hz, 1 cycle deg^{-1} gratings on green field

The drifting grating had different amplitude ratios of L' and M' contrast, either positive or negative. For the points (□) fitted by straight lines, the drifting M stimulus component led the L component by 80 deg spatial phase to compensate for the ~80 deg M' signal lag. For the points (○) fitted by the ellipse, the L and M components were summed spatially in phase or antiphase (not phase corrected). The ellipse is fitted with two parameters for LUM: $\phi = 80$ deg (the intrinsic L' *versus* M' phase shift) and $a/b \approx 2{\cdot}2$ (ratio of L' and M' contrast weights). The average S.E.M. of the data points is 9%, with a maximal value of 16%.

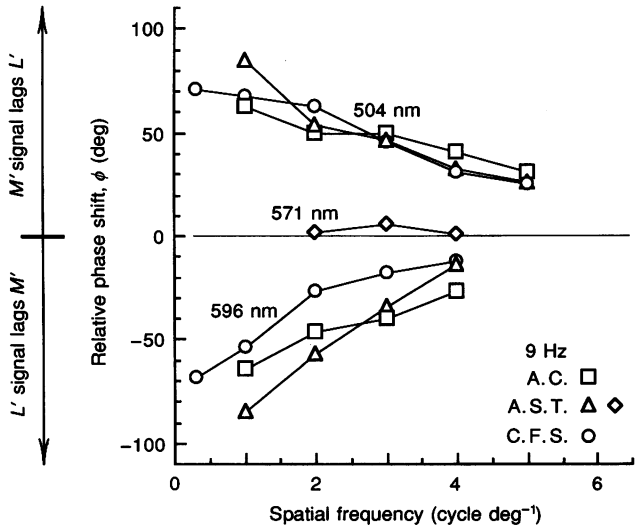

Figure 7. Phase shift between L' and M' signals in LUM at 9 Hz as a function of spatial frequency

The phase shifts on the green (504 nm) and orange (596 nm) fields are greatest at the lowest spatial frequency, but are clearly present at higher spatial frequencies. The phase shift is approximately zero on the green–yellow field (571 nm).

and thus give little net response (Enroth-Cugell & Robson, 1966). The substantial residual phase shift we observed on the green field at 4–5 cycle deg^{-1} suggests that the spatial frequency is not high enough to eliminate the surround response in the fovea. The motion of these relatively fine, 9 Hz patterns may be detected via the MC ganglion cells, since the quadrature protocol by enhancing motion sensitivity may isolate the MC pathway at spatial and temporal frequencies otherwise detected by the PC pathway (Merigan *et al.* 1991).

The difference in the fall-off of the phase shift (Fig. 7) with spatial frequency on the green *versus* orange field suggests that the surround diameter is different on these two fields. These results will be used to estimate the surround diameters after presentation of the model.

Effect of temporal frequency on the LUM phase shift. The effect of temporal frequency was assessed with patterns of 1 cycle deg^{-1}, since the phase shifts are large at this low spatial frequency. On the green–yellow field (Fig. 8, ◇) the phase shift was near zero at all temporal frequencies. There

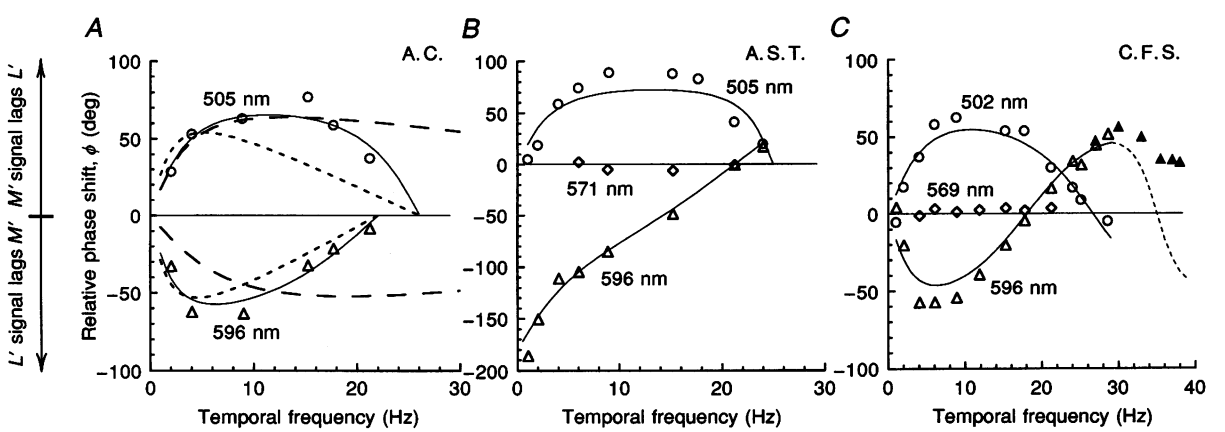

Figure 8. Phase shift between L' and M' signals in LUM at 1 cycle deg^{-1} as a function of temporal frequency

On the green field (○) the phase shift is similar for the three observers. On the orange field (△, ▲), the phase shift approaches 0 deg at the lowest temporal frequency for observers A.C. and C.F.S., but approaches 180 deg for A.S.T. On the green–yellow field (◇) the relative phase shift is near zero. The continuous curves show the fit of the receptive field model of MC ganglion cells. Parameters for A.C., A.S.T. and C.F.S., respectively: green field: $L_s/L_c = -0{\cdot}70$, $M_s/M_c = 0{\cdot}51$; $L_s/L_c = -0{\cdot}71$, $M_s/M_c = 0{\cdot}76$; $L_s/L_c = -0{\cdot}62$, $M_s/M_c = 0{\cdot}40$; orange field: $L_s/L_c = 0{\cdot}24$, $M_s/M_c = -0{\cdot}75$; $L_s/L_c = 0{\cdot}20$, $M_s/M_c = -1{\cdot}86$; $L_s/L_c = 0{\cdot}20$, $M_s/M_c = -0{\cdot}61$. For observer A.C., the dotted curves show best fit of the model without the facilitory surround: green field: $L_s/L_c = -0{\cdot}81$, $M_s/M_c = 0{\cdot}0$; orange field: $L_s/L_c = 0{\cdot}0$, $M_s/M_c = -0{\cdot}81$; and the dashed curves show the best fit with a short 5 ms surround delay: green field: $L_s/L_c = -0{\cdot}90$, $M_s/M_c = 0{\cdot}0$; orange field: $L_s/L_c = 0{\cdot}0$, $M_s/M_c = -0{\cdot}79$. L_s and L_c, L centre and surround, respectively; M_s and M_c, M centre and surround, respectively (see text and legend to Fig. 14).

is thus a rather precise field wavelength that induces no L' *versus* M' phase shift in LUM for all spatial and temporal frequencies tested (Figs 7 and 8). On the green field (○) the phase shift was small at 1 Hz; it grew with increasing temporal frequency (with a broad peak at 9–15 Hz) and then decreased at higher frequencies reaching 0 deg at ~26 Hz. On the orange field (△), the phase shift decreased above 12 Hz crossing zero near 20 Hz, and strongly reversed at higher frequencies. At low temporal frequencies the phase shift decreased for observer A.C. and C.F.S. (approaching 0 deg near 1 Hz), but for observer A.S.T. the phase shift surprisingly accelerated towards 180 deg between 4 and 1 Hz. This 'reversed' phase shift at low temporal frequency will be examined further.

The results at higher frequencies from 25–38 Hz on the orange field (observer C.F.S; Fig. 8*C*, ▲) were obtained with a modified display (having a higher frame rate of 200 Hz and a reduced raster size to achieve greater display monitor luminance and hence higher contrast (mean field, 1600 td)). The phase shift on the orange field reached a peak of ~55 deg at 30 Hz and descended slightly at higher frequencies. The curves show the prediction of our receptive field model.

The 1 cycle deg^{-1} patterns were also used to measure the phase shifts with the flicker discrimination protocol on the green and orange fields. The L test and M test were separately added to the luminance pedestal *spatially in phase*, producing pure flicker with no net motion. As in the quadrature motion protocol, the relative phase shift between the L' and M' signals is specified by the difference of the temporal phase settings that produce flicker nulls for the L test and the M test. The phase shifts (Fig. 9) assessed with flicker were nearly identical to those obtained with the motion criterion (dashed lines show the motion data from Fig. 8). Similar phase shifts were also measured (observer C.F.S.) with 9 Hz uniform flicker (3·5 deg diameter): the M' signal lagged L' by 78 deg on the green field, and L' lagged M' by 75 deg on the orange field.

It may seem surprising that the phase shifts are the same for flicker and motion. For the flicker protocol the patterns are spatially in phase, so flicker strength may be judged locally at the spatial peaks of the grating. For motion the two flickering patterns are separated 90 deg in spatial phase, so comparisons may be made more globally. The phase shifts will be identical for flicker and motion if the phase shifts arise in the retina, with the higher motion mechanisms simply assessing whether the L' and M' retinal signals are in temporal synchrony, at the motion null. Levinson & Sekuler (1975) concluded that motion and flicker are detected by the same mechanism on the basis of a comparison of detection thresholds for counterphase *versus* moving gratings.

Relative L' and M' contrast weights in LUM

The relative L' and M' weights may vary strongly with temporal frequency on coloured fields which produce large phase shifts (even when the pedestal and test are combined in optimal spatial–temporal phase). The receptive model of MC ganglion cells will show how the phase shifts and changing contrast weights arise simultaneously.

The relative L' and M' weights were assessed in three ways. First, motion contrast thresholds were measured in the quadrature protocol for the L test and the M test combined in *optimal* phase with the luminance pedestal. Second, motion nulls in the quadrature protocol were measured for

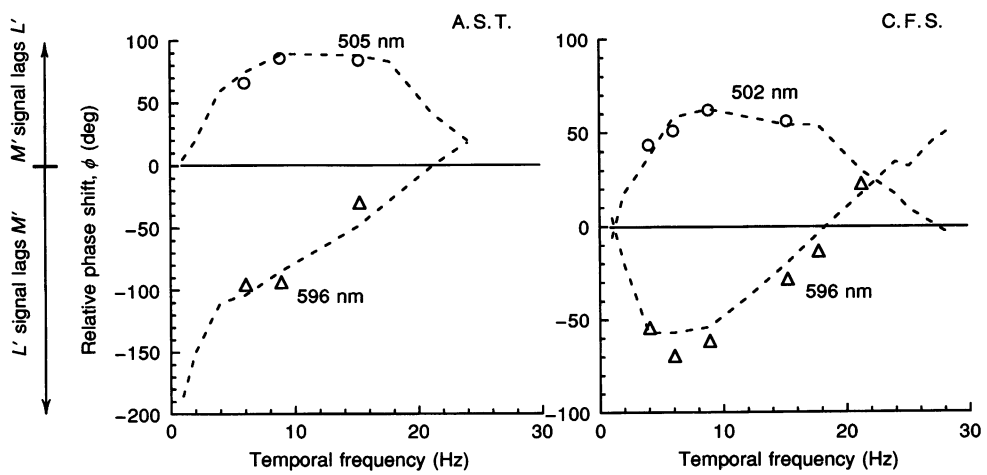

Figure 9. Phase shift between L' and M' signals in LUM at 1 cycle deg^{-1} in flicker discrimination protocol

The observer attempted to choose the test interval with greater apparent luminance flicker ('agitation'). The stimulus produces pure flicker with no motion, since the flickering pedestal and test are spatially in phase. The dashed lines, from the quadrature motion protocol (Fig. 8), show that the phase shift is highly similar for motion or flicker.

tests covering the full range of stimulus vector angles in the L', M' co-ordinates, each paired with the common luminance pedestal; the relative contrast weights and phase shifts are extracted from the nulls. Third, the weights were directly deduced from the earlier phase shifts measured in the quadrature protocol. The three methods gave fairly consistent weight estimates. The contrast weights were measured with the 1 cycle deg^{-1} patterns so the weights could be compared with the phase shifts for the same patterns.

First method: weights at the optimal phase for motion. We originally measured motion nulls for the L test and M test combined with the luminance pedestal. The pedestal and test are always maintained in spatial quadrature. The optimal condition for motion then occurs when the test is added to the pedestal at a temporal phase 90 deg away from the null temporal phase, so pedestal and test are in *effective* spatial–temporal quadrature. Contrast motion direction thresholds were measured for the L test and the M test added to the luminance pedestal in this optimal phase. This corresponds to measurement of the test contrast threshold at the trough of the phase template where sensitivity is greatest (Stromeyer *et al.* 1995). The relative L' and M' contrast weights (a/b) were specified by the inverse ratio of the L and the M test contrast thresholds.

Figure 10 (○) shows the relative L' and M' weights measured in this manner. The weights changed markedly with temporal frequency, in opposite directions on the green *versus* orange field. On the green field the M' signal, or weight, was greater than L' at low temporal frequency, but the L' signal became strongly dominant at high frequency.

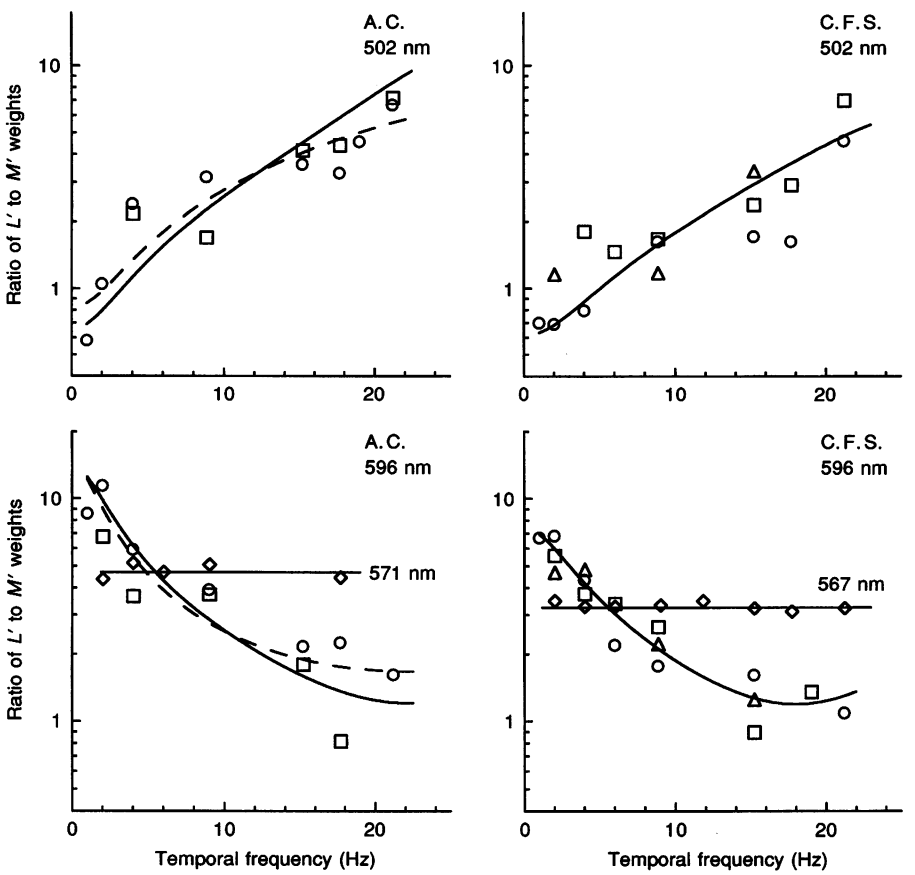

Figure 10. Ratio of L' and M' contrast weights in LUM as a function of temporal frequency
Weights measured with quadrature motion protocol with patterns of 1 cycle deg^{-1} on the green, green–yellow and orange fields. The relative weights were assessed in several ways (see text): from motion contrast thresholds for the L test and M test added to the luminance pedestal in optimal phase (○); from the 'minimum motion method' on the green–yellow field (◇); from the motion nulls (Fig. 11) for tests at many different L', M' cone-contrast vector angles added to luminance pedestal (△); from the temporal phase shifts of the L test and the M test relative to the luminance pedestal needed for the motion nulls (□). The average S.E.M. of the data indicated by ○ is 15 and 12% for observers A.C. and C.F.S., respectively, with a maximal value of 26 and 24%, respectively. Curves show model fit derived from the phase results, with the *length* of the L phasors components (L_c and L_s) scaled relative to the M components (M_c and M_s) by these factors: observer A.C. and C.F.S., respectively: green field, 3·3 and 2·25; orange field, 2·8 and 2·4. The dashed curves for A.C. show the best fit with the short 5 ms surround delay; the L phasors were scaled relative to M by 8 and 3·0 on the green and orange fields, respectively.

On the orange field the L' signal was highly dominant over M' at low frequency, and the L' and M' signals were nearly equal at 21 Hz.

Our model attributes the large change in contrast weights to an interaction of the centre and surround of the MC receptive field. If the surround is important for the large changes in relative weights, then the weights should change much less with fine patterns. The relative weights were measured at 4 cycle deg^{-1} and 4 Hz on the green and orange fields, a temporal frequency that produced large changes in the contrast weights on the green and orange field at 1 cycle deg^{-1} (Fig. 10). The weight ratio (a/b) was quite similar for the 4 cycle deg^{-1} patterns on the green and orange fields: 3·3 and 3·9, respectively, for observer A.C. and 2·8 and 2·7, respectively, for observer C.F.S. The ratio was 2·3 and 2·7, respectively, on the green and orange field (observer C.F.S.) for the 4 cycle deg^{-1} patterns at a lower temporal frequency of 1 Hz. This reduced weight variation with these fine patterns supports the role of the receptive surround in the model.

The relative weights for the 1 cycle deg^{-1} patterns were essentially constant with temporal frequency on the green–yellow field (Fig. 10, ◇) that produces no phase shift. Just before these measurements, we assessed the particular green–yellow field wavelength for each observer which produced no phase shift at 9 Hz. The relative contrast weights were then determined by combining a supra-threshold test and a luminance pedestal in spatial–temporal quadrature, and varying the test vector angle in the L', M' co-ordinates to find the motion null (50% point on the frequency-of-seeing curve); this is the minimum motion method of Anstis & Cavanagh (1983). This specifies the equiluminant axis (Anstis & Cavanagh, 1983) lying parallel to the slope of the LUM detection contour in the L', M' co-ordinates (Stromeyer *et al.* 1995). The minimum motion method accurately specifies the equiluminant axis only when there is no appreciable L' *versus* M' phase shift in LUM, as a phase shift will bias the setting (Stromeyer *et al.* 1995). The fact that relative weights are essentially *constant* suggests that a single mechanism, LUM, is isolated. The quadrature protocol thus allows us to isolate the MC pathway even at frequencies as low as 2 Hz.

Second method: relative weights determined with tests at many vector angles in the cone-contrast co-ordinates. We present a new method for estimating in LUM the relative L' and M' weights (a/b) and intrinsic phase shift (ϕ) from the motion nulls for the full range of tests in the L', M' co-ordinates, each combined in spatial quadrature with the luminance pedestal. The method is mathematically based on an extension of our earlier analysis of the quadrature motion protocol (Stromeyer *et al.* 1995). Lee, Martin, Valberg & Kremers (1993) made related measurements on single retinal MC cells: the response to flicker was assessed for tests covering the full range of angles in the L', M' co-ordinates. We show how the full range of test vectors in our experiment can be used to estimate the two parameters ϕ and a/b; the good fit obtained suggests that a single pathway, LUM, signals all the stimuli.

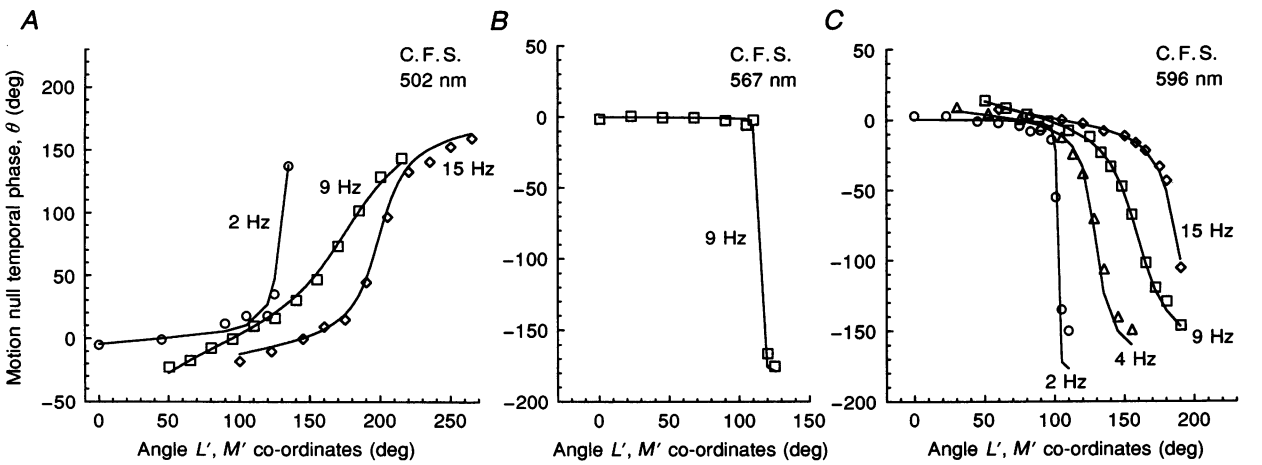

Figure 11. Relative stimulus phase (θ) for motion nulls in quadrature motion protocol for tests at many stimulus vector angles in the L', M' cone-contrast co-ordinates

Motion nulls are shown for several temporal frequencies of the 1 cycle deg^{-1} gratings on green (*A*), green–yellow (*B*) and orange (*C*) adapting field of 1300 td. Each test was paired with the luminance pedestal. For clarity, on the green field the 9 and 15 Hz curves are displaced rightward 50 and 100 deg; on the orange field the 4, 9 and 15 Hz curves are displaced rightward 30, 50 and 60 deg, respectively. The relative L' and M' intrinsic phase shift, ϕ, and relative contrast weights, a/b, were estimated from the fitted curves: 502 nm field: 2 Hz: 10 deg, 1·16; 9 Hz: 61 deg, 1·19; 15 Hz: 60 deg, 3·4; 567 nm field: 9 Hz: 0 deg, 2·3; 596 nm field: 2 Hz: −2 deg, 4·7; 4 Hz: −40 deg, 4·8; 9 Hz: −44 deg, 2·3; 15 Hz: −21 deg, 1·26.

Figure 11 shows the temporal phase of the test, θ, relative to pedestal that produces a motion null for tests covering a wide range of vector angles in the L', M' co-ordinates. Each point (motion null) is based on a frequency-of-seeing curve. On the green–yellow field (Fig. 11*B*) the data show a steep step, indicating that the motion sharply reverses direction as the test is rotated through the equiluminant axis in the L', M' co-ordinates (Anstis & Cavanagh, 1983). A steep step is expected if there is no intrinsic phase shift between the L' and M' signals ($\phi = 0$ deg) and there is little interunit variability in the equiluminant points of the cells comprising LUM (Cavanagh & Anstis, 1991). The fitted curve indicates that $\phi = 0$ deg on this field. On the green (Fig. 11*A*) and orange (Fig. 11*C*) fields, the intrinsic phase shift causes the functions to reverse more gradually. The functions are especially gradual at 9 Hz where we expect a large phase shift.

Curves were fitted to extract the relative weights, a/b, and intrinsic phase, ϕ (parameters are listed in the legend and the relative weights are shown in Fig. 10, △). The analysis extends our previous discussion of the quadrature motion protocol (Stromeyer *et al.* 1995). The phasors in Fig. 12 represent the magnitude (phasor length) and relative phase (phasor angle) of the L' and M' LUM signals produced by the flickering pedestal and test, referenced to a *fixed* retinal point. The phasors rotate one cycle for each cycle of the periodic stimuli. The counterphase pedestal and test each have equivalent left *and* right moving components. The LUM signal produced by the pedestal is depicted by the same pedestal phasor P_{right} or P_{left}, since the left and right motions are identical, from the vantage of a fixed retinal point. Phasor P is the vector sum of the weighted LUM contrast signals aL'_{p} and bM'_{p}. In this example the L' signal lags M' by the intrinsic phase shift ϕ (a lag is represented by *clockwise* rotation).

Perceived motion is produced by an interaction of signals from the pedestal and test. To predict the net left–right luminance motion we must consider the combined pedestal

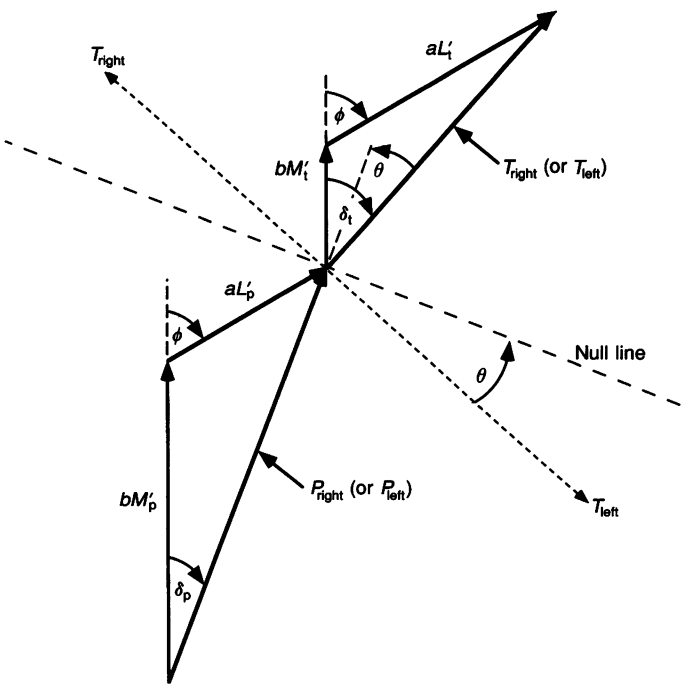

Figure 12. For analysing results of Fig. 11, a phasor analysis of the quadrature motion protocol was used to assess in LUM the intrinsic phase shift (ϕ) and relative L' and M' weights (a/b)

The counterphase pedestal and test each have equivalent left- and right-moving components. The counterphase luminance pedestal signal, P, is shown here with the LUM weighted aL'_{p} signal physiologically lagging bM'_{p} by ϕ. Parameters ϕ and a/b are the same for pedestal and test since they reflect properties of LUM. These parameters were estimated from the motion nulls (Fig. 11) for the test set to different stimulus vector angles in the L', M' cone-contrast co-ordinates; this changes the ratio of test contrast components, aL'_{t} and bM'_{t}. The counterphase test, T, is first represented by solid phasors for the test *stimulus* in phase spatially and temporally with the pedestal. In the experiment the test was in spatial quadrature with the pedestal, causing the left- and right-moving test components to shift 90 deg in opposite directions (dotted phasors). This latter flickering test pattern must be temporally advanced by θ to lie on motion null line (orthogonal to the pedestal phasor) where the left *versus* right motion of pedestal-plus-test is balanced. To simplify analysis, we imagine the test is spatially in phase with the pedestal; the temporal phase shift, θ, then makes the original test T (solid phasor) *collinear* with the pedestal phasor.

and test signals. Phasor T is the vector sum of the LUM test signals, aL'_t and bM'_t. The parameters a/b and ϕ (the relative weights and intrinsic phase shift) are the same for pedestal and test since they reflect properties of LUM. The luminance pedestal has a fixed spectral composition (represented by a 45–225 deg vector in the L', M' co-ordinates), but the test is set to many different stimulus vector angles in the L', M' co-ordinates. Hence the relative lengths and signs of the test components, aL'_t and bM'_t, will change with the test vector orientation in the L', M' co-ordinates.

The solid phasor T depicts the test signal for the test stimulus first presented *spatially and temporally in phase* with the pedestal stimulus. However in the experiment, the test is presented in quadrature spatial phase with respect to the pedestal; this causes the left and right test phasors to rotate 90 deg in opposite directions (shown by the dotted phasors). A motion null occurs when these two dotted test phasors lie on the 'null line', *orthogonal* to the pedestal phasor, for then the *total* left and right motion of pedestal-plus-test is balanced. As shown, the test stimulus must be *temporally* phase shifted by θ deg to lie on the null line. A trick can be used to simplify the analysis: imagine that there was no quadrature spatial phase shift (i.e. the pedestal and test stimuli are presented spatially in phase, as first depicted by solid phasor T). In this case the same stimulus temporal phase shift, θ, will make T *collinear* with the pedestal phasor P (as shown by the dashed line collinear with phasor P). The motion nulls for a wide range of tests in the L', M' co-ordinates (Fig. 11) were used to estimate the values of a/b and ϕ which provided the best approximation of this collinear relation.

To estimate a/b and ϕ, the curves in Fig. 11 were fitted as follows using a least-squares criterion. The pedestal phasor P_{right} (or P_{left}) in Fig. 12 can be expressed by unit vectors i_x and i_y in Cartesian co-ordinates, with coefficients:

$$P_{\text{right,x}} = aL'_p \sin\phi,$$

$$P_{\text{right,y}} = bM'_p + aL'_p \cos\phi,$$

where $P_{\text{right}} = P_{\text{right,x}} i_x + P_{\text{right,y}} i_y$ and ϕ is the relative phase lag of the L signal. The test phasor T_{right} (or T_{left}) is defined in a similar way.

From trigonometry, the angles δ_p and δ_t (Fig. 12) are:

$$\delta_p = \arctan(aL'_p \sin\phi / (bM'_p + aL'_p \cos\phi)),$$

$$\delta_t = \arctan(aL'_t \sin\phi / (bM'_t + aL'_t \cos\phi)).$$

The pedestal has a fixed angle of 45 deg in the L', M' co-ordinates, hence $L'_p = M'_p = 1$. The above expressions can be rewritten:

$$\delta_p = \arctan(\sin\phi / (C + \cos\phi)),$$

where C is the inverse of the L and M weight ratio, a/b; similarly,

$$\delta_t = \arctan(\sin\phi / (C\tan\gamma + \cos\phi)),$$

where $\tan\gamma = M'_t/L'_t$. The parameter γ represents the test angle in the cone-contrast co-ordinates; this was varied in the experiment. The stimulus temporal null phase, θ, measured in the experiment is simply the difference $\delta_t - \delta_p$ (Fig. 12); thus:

$$\theta = \arctan(\sin\phi / (C\tan\gamma + \cos\phi)) - \arctan(\sin\phi / (C + \cos\phi)).$$

Third method: contrast weights determined from the phase shifts for the L and M test. The third method assesses the relative L' and M' weights from the phase shifts previously measured for the L test and M test separately combined with the luminance pedestal in the quadrature protocol. If the L test is shifted in temporal phase by β deg (relative to the luminance pedestal) to achieve a motion null, and the M test is shifted by α deg, then the relative contrast weights (Stromeyer *et al.* 1995) are given by:

$$aL'_p / bM'_p = (\sin|\alpha| / \sin|\beta|).$$

This can be understood intuitively. Suppose the response to the luminance pedestal is strongly dominated by L cones, i.e. large L' weight. The luminance pedestal will then act much like an L pedestal, so little phase shift would be expected for the L test, but a large phase shift would be expected for the M test provided there was in fact a large intrinsic L' *versus* M' phase shift. Thus, a large phase shift for the M test and a small shift for the L test implies a large L weight and a small M weight. The relative weights determined by this method are shown in Fig. 10 (□).

Retinal model of the LUM phase shift and relative contrast weights

Physiological recordings indicate that the large relative phase shifts arise in the retinal MC ganglion cells (Smith *et al.* 1992). We propose a simple model of MC cells to explain both the phase shifts and changing contrast weights. The model is based on a linear centre-surround receptive field, but chromatic adaptation is assumed to modify the spectral nature of the surround to account for the reversed phase shift on green and orange fields. Derrington & Lennie (1984) observed that most MC cells show linear spatial summation between centre and surround. Smith *et al.* (1992) proposed a linear model to explain the phase shift for orange adaptation. Our model has two unusual features: the spectral nature of the surround changes with chromatic adaptation and the surround delay is quite long. We first consider the model assuming that there is *no latency difference* between the L and M photoreceptor signals *per se*, as in the model of Smith *et al.* (1992).

Following Enroth-Cugell, Robson, Schweitzer-Tong & Watson (1983), we use phasors to represent the response of centre and surround to sinusoidal luminance modulation; phasor length specifies response magnitude and phasor angle specifies response phase. Figure 13 adopted from Enroth-Cugell *et al.* (1983) shows the response of an on-centre cell. The vertical phasor represents the centre response (arbitrarily plotted vertically). The surround response, of opposite sign, would be represented by a downward vertical phasor, but owing to the surround delay the phasor is rotated slightly clockwise by ρ. The 'cell response' is the vector sum of centre and surround phasors. The cell response is advanced in phase owing to the delayed surround, as shown by the anticlockwise rotation of the cell response relative to the centre. This phase advance is clearly

seen in MC cells (Lee *et al.* 1994); at low spatial and temporal frequencies the cell response to luminance flicker is considerably advanced relative to the flicker.

To make the model simple, we adopt two features of the model of Enroth-Cugell *et al.* (1983), which described well the response of cat X ganglion cells measured up to 32 Hz: (1) the ratio of responsivity of centre-to-surround is independent of temporal frequency over the range of our measurements (typically 1–25 Hz), and (2) the surround has a constant delay (in milliseconds) relative to the centre. Point (1) implies that the ratio of the lengths of the centre and surround phasors does not change with temporal frequency, while point (2), the fixed surround delay, implies that with increasing temporal frequency the surround phasor will shift proportionally clockwise relative to the centre phasor. Enroth-Cugell *et al.* (1983) also considered a model with more complex features, such as a single low-pass stage for the surround.

On-centre MC cells (Fig. 14) summate L and M signals in their centre (Lee, Martin & Valberg, 1988). Smith *et al.* (1992) emphasized that, if the centre and surround have the same spectral sensitivity, there will be *no* phase shift between the L and M signals of the cell in response to luminance flicker, regardless of the surround delay. The spectral sensitivity of the centre appears to be relatively constant on different coloured adapting fields (Lee *et al.* 1988). Thus to explain the large L' *versus* M' phase shifts which change with adapting field colour, we must assume that chromatic adaptation modifies the spectral nature of the surround causing it to be different from the centre, and the surround must be different on green *versus* orange fields. In addition, there must be a delay between the centre and surround; without a surround delay or lag there can be no relative phase shift between the L' and M' signals.

The L and M response components of the cell are represented independently (Fig. 14), as though there are two superposed receptive fields: one with L centre and surround (L_c and L_s) and the other with M centre and surround (M_c and M_s). This is based on the assumption of linear independence of the L and M signals (Derrington *et al.* 1984). In Fig. 14, the L and M centre responses to the luminance flicker are in phase, arbitrarily represented by upward vertical phasors. Figure 14*A* shows how orange adaptation is supposed to modify the receptive field surround. At low temporal frequencies, orange adaptation causes the M surround to be antagonistic to the centre, but the sign of the L surround is reversed and is thus 'facilitory'. (This sign inversion between the L and M surround components is needed to fit the phase data, as shown later.) Orange adaptation thus makes the surround of type +L−M. This was confirmed by the physiological measurements of Smith *et al.* (1992). Owing to the surround delay, the antagonistic and facilitory surround phasors, M_s and L_s, are rotated clockwise by equal amounts (by ρ deg phase from vertical); the two surround phasors are thus collinear but of opposite sign.

The L' signal of the cell in response to the luminance flicker (Fig. 14) is specified by L_{sum}, the vector sum of the L centre and surround phasors, L_c and L_s. Similarly, the M' signal of the cell to luminance flicker is specified by the M_{sum} phasor. The phase shift between the L' and M' signals of the cell is specified by *only* the angle between the sum phasors, L_{sum} and M_{sum}, and is thus independent of the relative magnitude of the two separate *sum* phasors. As shown in Fig. 14*A*, on the orange field the L' signal strongly lags M'. The opposite phase shift on the green field (Fig. 14*B*) can be obtained by simply reversing the spectral signs of the surround components, to form a surround of type +M−L. Thus chromatic adaptation changes the sign and the relative

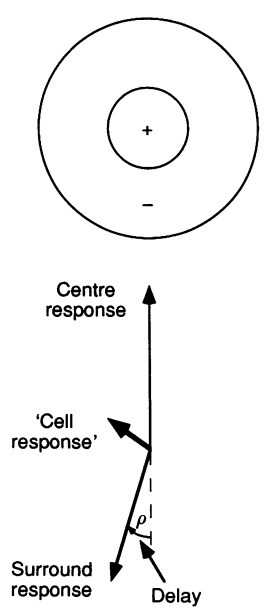

Figure 13. Phasor representation of the response of on-centre retinal ganglion cell to uniform luminance flicker

This figure, adopted from Enroth-Cugell *et al.* (1983), shows the magnitude and relative phase of the response components, represented by phasor length and angle, respectively. The response of the excitatory receptive field centre is arbitrarily plotted vertically. The response of the antagonistic surround (of opposite sign) is plotted as a downward phasor, rotated clockwise by ρ deg to reflect the surround delay. The 'Cell response' is the vector sum of centre and surround responses.

weights of the L and M *surround* components. Off-centre cells predict the same phase shift, assuming that all phasor components in Fig. 14 are simply inverted (Smith *et al.* 1992).

Model fit of *L′ versus M′* LUM phase shift. To fit the phase data, we independently varied the angle of the L and the M sum phasors by changing the relative length and sign of the surround components (L_s and M_s). The centre components, L_c and M_c, were arbitrarily equated in length. There were thus three parameters for the fit: the signed ratios L_s/L_c and M_s/M_c and the surround delay, ρ. These parameters were fixed for each adapting condition. (The spatial frequency was fixed at 1 cycle deg^{-1}.) The surround delay is assessed from the high temporal frequency at which the relative phase shift *goes through zero*. The required delay is quite large (~20 ms) to account for the fact that the *L′ versus M′* signal phase shift goes through zero near 20 Hz on the orange field and 26 Hz on the green field (Fig. 8). At these particular frequencies the large delay causes both surround phasors (L and M) to 'catch up' and become *collinear* with the two centre phasors, thus producing zero relative phase shift (i.e. 0 deg difference between the L and M *sum* phasors).

The phase results were fitted as follows. The phasor L_{sum} can be expressed in Cartesian form as:

$$L_{sum} = L_{sum,x} i_x + L_{sum,y} i_y,$$

with coefficients:

$$L_{sum,x} = -L_s \sin\rho,$$

$$L_{sum,y} = L_c - L_s \cos\rho,$$

and similarly for M_{sum}. Angle ρ (Fig. 14) specifies the surround delay in degrees (i.e. the product of the delay in deg Hz^{-1} and temporal frequency in Hz).

The scalar product of vectors L_{sum} and M_{sum} is:

$$L_{sum} \bullet M_{sum} = |L_{sum}||M_{sum}| \cos\phi,$$

where ϕ is the *L′ versus M′* phase shift, i.e. the angle between the two sum phasors. Solving for ϕ yields:

$$\phi = \arccos\left(\frac{M_c L_c + M_s L_s - M_c L_s \cos\rho - M_s L_c \cos\rho}{(M_c^2 + M_s^2 - 2M_c M_s \cos\rho)^{1/2}(L_c^2 + L_s^2 - 2L_c L_s \cos\rho)^{1/2}}\right).$$

To determine the phase shift ϕ, we need to estimate only the ratios L_s/L_c and M_s/M_c. We thus set $L_c = M_c = 1$, and simplify the equation:

$$\phi = \arccos\left(\frac{1 + M_s L_s - L_s \cos\rho - \cos\rho}{(1 + M_s^2 - 2M_s \cos\rho)^{1/2}(1 + L_s^2 - 2L_s \cos\rho)^{1/2}}\right).$$

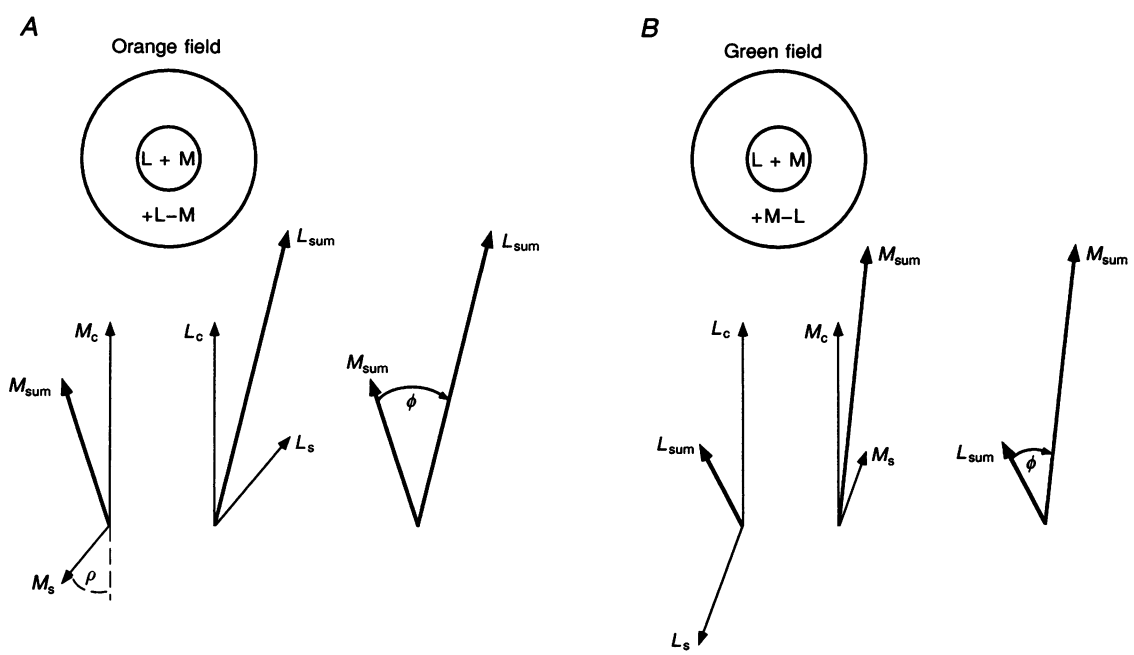

Figure 14. Phasor representation of the modelled response of on-centre MC retinal ganglion cells on orange (*A*) and green (*B*) adapting fields

The L and M response phasors are shown separately. The centre summates L and M signals. Chromatic adaptation modifies the surround; on the orange field at low temporal frequency the M surround is antagonistic to the centre, but the L surround, of opposite sign, is facilitory. The L and M surround components are reversed in sign on the green field. Both L and M surround components are delayed by ρ deg relative to the centre (i.e. collinear but of opposite sign). The L and M responses of the cell to luminance flicker are represented by the sum phasors, L_{sum} and M_{sum}, respectively. The angle between L_{sum} and M_{sum} represents the *L′ versus M′* intrinsic phase shift in LUM (ϕ), and the ratio of lengths of L_{sum} and M_{sum} represents the relative *L′* and *M′* contrast weights (a/b). The phasors depicted here were used to fit the phase data for observer C.F.S. (Fig. 8), shown with the delay at 3 Hz.

The continuous curves in Fig. 8 show the model fit of the phase shift on the green and orange fields, with the parameters specified in the legend. The dotted curves (Fig. 8*A*) depicted for observer A.C. show why we need a facilitory surround component. These dotted curves show the best fit *without* the facilitory surround component; to eliminate the facilitory surround components we set the L_s phasor on the orange field and the M_s phasor on the green field to zero length. The predicted phase shift rises to a maximum near 5 Hz but then descends too rapidly. Smith *et al.* (1992) also rejected such a model with an antagonistic surround fed by a single cone type, L or M. Figure 14 shows the phasors actually used to fit the results for observer C.F.S. on the green and orange fields, with the surround delay (i.e. surround phasor angles) depicted for 3 Hz.

The model requires a rather large surround delay. If instead we assumed a delay of ~5 ms, like the surround delay estimated by Smith *et al.* (1992) for red–green PC retinal ganglion cells, then the phase shift (Fig. 8*A*, dashed curves) rises to a maximum at 5–10 Hz, where it reaches a plateau and does not descend to zero until 100 Hz. Smith *et al.* (1992) assumed that the surround response becomes 'achromatic' like the centre at high temporal frequencies (e.g. > 10 Hz); thus the spectral opponency disappears. This could potentially explain the reduced phase shift at high frequencies, since the relative phase shift would vanish if the centre and surround have matched spectral sensitivity. However, to explain the large changes in relative contrast weights above 10 Hz, we need L and M opponency in the surround at temporal frequencies at least as high as 20 Hz; spectral opponency thus does not disappear (as supported by later results). Thus the small phase shift near 20 Hz may be caused by the large surround delay, not by the disappearance of the spectrally opponent surround.

Model fit of relative L' and M' contrast weights in LUM. The relative phase shift is specified by only the angle between the separate sum phasors, L_{sum} and M_{sum}, and is thus unaffected by a relative size scaling of the L and M sum phasors. The relative L' and M' weights are specified by the ratio of *lengths* of the two sum phasors, L_{sum}/M_{sum}, at each temporal frequency. The model prediction of these relative weights (a/b) is shown by the curves in Fig. 10. The shape of the curves in these co-ordinates is determined from the above fits of the phase data. To fit the relative weights, we simply slide these curves of fixed shape vertically along the log a/b weight axis (the scaling factors are specified in the legend to Fig. 10). In fitting the phase data, the length of the centre phasors was arbitrarily equated, $L_c = M_c = 1$. To fit the relative weights, the length of the L phasor components (L_c and L_s) are scaled up by the *same* factor (~3-fold) relative to the M components (M_c and M_s).

This indicates that the L photoreceptor signal contribution to LUM is ~3 times that of M. This factor of three also approximately describes the relative L' and M' weights at higher spatial frequencies on green and orange fields and for the yellow–green adapting conditions where there is no L' *versus* M' phase shift. This dominance of the L' signal in luminance motion detection has been observed by others (Gegenfurtner & Hawken, 1995; Stromeyer *et al.* 1995).

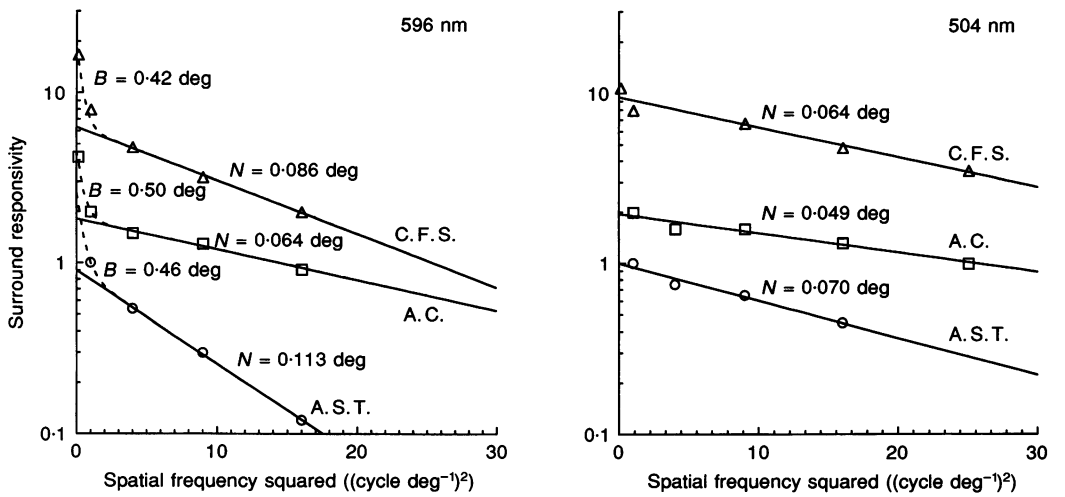

Figure 15. Estimations of the radius, r_s, of the receptive field surround from phase shifts at different spatial frequencies on orange and green fields (Fig. 7)

The $\log_{10}$ of surround responsivity is plotted *versus* the square of spatial frequency, since in such co-ordinates the results will fall on a straight line if the surround has a circular Gaussian weighting function (see text). The slope of the line then specifies the surround radius, r_s, designated beside each line. Both a narrow (N) and broad (B) component was estimated, with the dashed line representing the sum of the two components on orange field. Surround responsivity was estimated using the receptive field model of MC cells. Bottom curves in correct position, but the other two higher curves were shifted up 2-fold and 8-fold.

The phasors in Fig. 14 illustrate why the relative L' and M' weights change strongly with temporal frequency. On the orange field at low temporal frequency, M_c and M_s are of opposite sign so they partially cancel, but at high frequency (~20 Hz) the delayed M surround phasor has swung around to support the M centre phasor. The opposite occurs for L_c and L_s: at low frequency on the orange field the two phasors have the same sign and add, but at high frequency the L surround phasor has swung around to partially cancel the L centre phasor. Thus on the orange field the L' signal is much more effective than M' at low temporal frequency (Fig. 10), but at high frequency the two signals are comparable in effectiveness. The opposite changes in the weights is observed on the green field owing to the reversed signs of the L and M surround components.

The dashed lines in Fig. 10 show the prediction of the model based on the short, 5 ms surround delay. With the short delay the fits to the weights are good, but the phase fits are extremely poor (Fig. 8*A*). Moreover to fit the weights on the green field with the short delay, the L phasors must be scaled by a large, unrealistic amount (8-fold) relative to the M phasors (Fig. 10, see legend). The model with the longer surround delay provides a reasonable fit to both the phase shifts and relative weights.

Estimation of the size of the receptive field surround. The model assumes that the surround is important for the phase shift. We can now estimate the size of the surround from the earlier measurements of the phase shift (Fig. 7) at different spatial frequencies. The phase shift fell off with spatial frequency at different rates on the green and orange fields, suggesting that the surround size is different on the two fields. The original data are replotted in the new co-ordinates of Fig. 15 to better estimate the surround diameters, as explained in the following section.

As spatial frequency is raised, the surround response falls off faster than the centre response, which can be represented as a decrease in the length of the L and M surround phasors relative to the centre phasors. The model was previously fitted (Fig. 8) to the phase shifts measured at 1 cycle deg^{-1} over a wide range of temporal frequencies, on the green and orange fields. The *relative* surround responsivities for 1 cycle deg^{-1} are arbitrarily plotted at an ordinate value 1·0 in Fig. 15. To fit the phase shift at other spatial frequencies, the surround responsivity was allowed to vary (with the other model parameters fixed, as listed in the legend to Fig. 8). Figure 15 shows a plot of $\log_{10}$ of surround responsivity *versus* the square of the spatial frequency. In these co-ordinates data should fall on a straight line provided the surround has a circular Gaussian weighting function. Consequently, the surround radius can be estimated from the slope, as follows.

The responsivity of the Gaussian surround (R_s) as a function of spatial frequency (Enroth-Cugell & Robson, 1966) is represented:

$$R_s(v) = K_s \pi r_s^2 \exp(-(\pi r_s v)^2),$$

where v is spatial frequency (cycle deg^{-1}), K_s is peak sensitivity and r_s is the radius (deg) of the Gaussian surround. The expression can be rewritten:

$$y = \log_{10} R_s(v) = 0{\cdot}434 \ln(R_s(v)) = 0{\cdot}434(-(\pi r_s v)^2 + \ln(K_s \pi r_s^2)).$$

The slopes in Fig. 15 can then be represented:

$$\frac{dy}{dv^2} = 0{\cdot}434 \pi^2 r_s^2$$

(with the term $0{\cdot}434 \ln(K_s \pi r_s^2)$ specifying the intercept of the lines at zero spatial frequency), and thus the radius can be determined from the slope:

$$r_s^2 = \frac{1}{4{\cdot}28} \times \frac{dy}{dv^2}.$$

The estimated surround radius, r_s, is listed beside each curve in Fig. 15. On the green field the radius is 0·049–0·064 deg, and is somewhat wider on the orange field, 0·064–0·113 deg. These rather narrow components are labelled *N*. In addition, on the orange field there is evidence for a much broader surround component (*B*), reflected in the strong rise between 1 and 0·31 cycle deg^{-1} (the lowest spatial frequency). The dashed lines for the orange field show the summed effect of the narrow and broad surround components. The strong, broad component will be examined later.

Kremers *et al.* (1994) inferred the surround size from phase shifts in humans using small, flickering foveal orange fields (red and green mixture) on a dark background. For two observers the phase shift was abolished at the smallest spot size (0·3 deg) but was still present for a third observer. They estimated $r_s = 0{\cdot}29$ deg, by fitting a Gaussian directly to the magnitude of the phase shift *versus* spot diameter. This may largely reflect the broad component we observed on the orange field. Judging the flicker of these small bright spots is probably difficult compared with our procedure of judging motion on a large field to which the observer is well adapted. Their results imply that there should be little phase shift above 2 cycle deg^{-1} on the orange field; our results (Fig. 7) show that the phase shift is considerably reduced but clearly present. The variance in their data for the smallest spots may preclude seeing a surround contribution smaller than ~30%. Gratings may be better than spots for estimating the narrow surround component.

Physiology shows (Derrington & Lennie, 1984; Croner & Kaplan, 1995) that the receptive field centre radius of macaque retinal MC cells (extrapolated to central fovea) is 0·04–0·06 deg. Macaque physiology (Croner & Kaplan, 1995) indicates that the surround radius may be ~5 times the centre radius, but there is little data for central fovea. Such a surround would be wider than the narrow component we estimate.

Incorporating photoreceptor latency effects in the model. The model provisionally assumed that there was no latency difference between the L and M photoreceptors *per se*. The relative phase shift was quite different on green

versus orange fields; the phase shift passed through zero at ~26 and 20 Hz, respectively. We now show that incorporating a plausible latency difference has little effect.

Recordings of red–green PC cells on the orange field (Smith *et al.* 1992) indicate that the L photoreceptors may be at most 2 ms faster than the M photoreceptors. This faster L cone response on the orange field might be caused by greater light adaptation of L cones compared with M cones. We observed no L' *versus* M' phase shift in LUM on a field of ~570 nm at all temporal frequencies. Thus we might assume that there is no photoreceptor latency difference on this field, and L and M cones are about equally light adapted. Shifting to the green field increases the M/L mean stimulation ratio by 1·8, about the same amount that shifting to the orange field decreases the M/L ratio relative to 570 nm. Thus a photoreceptor latency effect may be of *equal* size on the green and orange fields, but of opposite sign, and thus cannot explain the different phase shifts on the two fields.

The latency effect can be incorporated as follows. As described earlier the latency effect produces a phase shift of opposite sign to that actually observed. To retain the original model we adjusted the phase *data* to compensate for a possible latency effect: we increased the measured phase shifts by a factor reflecting a differential latency between L and M of 2 ms and also a larger difference of 5 ms, suggested as an upper limit (Donner, Koskelainen, Djuspsund & Hemilä, 1995). To correct the data for the latency effect, we increased the phase shift proportional with temporal frequency over the range 1–28 Hz. The original model with no latency effect was then fitted to this corrected data. On the orange field, the model describes the corrected data equally well assuming either no latency difference or a 2 or 5 ms difference. However, on the green field, the residual error of the fit increased 2-fold with the 5 ms difference (the corrected phase shifts were too large for the model over the range 9–17·7 Hz). Thus while a 2 ms latency difference is compatible with the measurements, a 5 ms latency difference may be too large.

Increased response of spectrally opponent surround in LUM at very low spatial frequency

Two unusual features of our model are the long surround delay and the presence of the spectrally opponent surround at high temporal frequency (20 Hz). This is in contrast to the model of Smith *et al.* (1992), which assumes that the relative phase shift is 0 deg at ~20 Hz, because the surround becomes achromatic like the centre. We assume that the surround remains spectrally opponent at 20 Hz, so instead the lack of relative phase shift at 20 Hz can be ascribed to the long surround delay. As shown earlier (Fig. 8), if the spectrally opponent surround is clearly present at ~20 Hz, then there will still be a large relative phase shift at 20 Hz if we assume a short surround delay (5 ms). Thus the fact that the phase shift goes through zero at 20 Hz, despite the presence of the spectrally opponent surround, reinforces the long surround delay in the model.

The remaining measurements confirm the presence of the spectrally opponent surround at both 1 and ~20 Hz. There

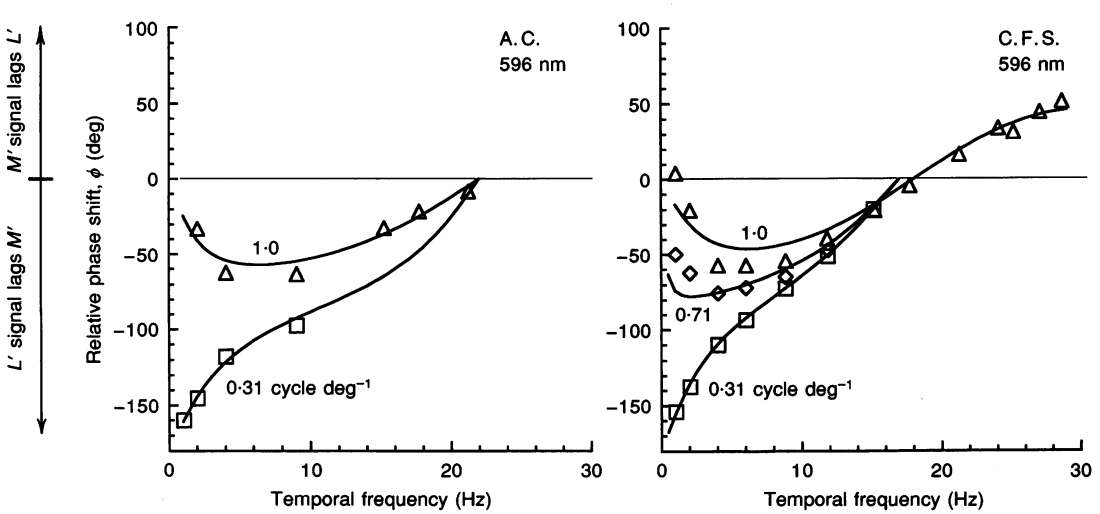

Figure 16. Phase shift between L' and M' signals in LUM on orange field as a function of temporal frequency, at 1 cycle deg^{-1} and lower spatial frequencies

Phase shift measured with quadrature motion protocol. At 0·31 cycle deg^{-1} the phase shift approaches 180 deg at low temporal frequency (as in Fig. 8 for observer A.S.T. at 1 cycle deg^{-1}). This inverted phase shift at low spatial frequency indicates L' and M' signals are summating negatively in LUM at low temporal frequency. The curves show the model fit: data for 1 cycle deg^{-1} redrawn from Fig. 8 (the legend to Fig. 8 specifies model parameters at 1 cycle deg^{-1}); for 0·31 cycle deg^{-1} the parameters were the same but the strength of the surround components were increased by 2·1- and 2·3-fold for A.C. and C.F.S., respectively; for 0·71 cycle deg^{-1} they were increased 1·57-fold.

is little disagreement about the presence of the spectrally opponent surround at low temporal frequency. Measurements were first made at 1 Hz to show that the spectrally opponent surround is augmented at spatial frequencies below 1 cycle deg^{-1}. We then used low spatial frequencies to show that the spectrally opponent surround is also present at 20 Hz, but its sign is reversed compared with low temporal frequencies owing to the long surround delay.

Measurements on orange field at low spatial and temporal frequency. We return to the low-temporal-frequency phase 'reversal' originally observed on the orange field (Fig. 8*A*). As mentioned previously, the phase shift for observer A.S.T. measured at 1 cycle deg^{-1} approached 180 deg at zero temporal frequency, indicating that LUM was responding to the difference of the L' and M' signals. (At low temporal frequencies the relative phase shift will approach 0 deg if the L' and M' signals summate positively within LUM, but if the signals summate negatively in a spectrally opponent manner then the phase shift will approach 180 deg.)

The reversal can be intuitively appreciated with the following observation: we presented the 1 cycle deg^{-1} luminance pedestal and M test, flickering in spatial–temporal quadrature at 1–3 Hz. Observer A.S.T. saw the motion in the reversed direction compared with the other two observers, and all observers saw strong motion. Thus for A.S.T., the reversed motion and the 'reversed' phase shift indicate that the M' signal is feeding into LUM with the opposite sign of L'. Stockman & Plummer (1994) observed a related effect.

The observer A.S.T. saw the motion in the *non*-reversed direction in the above protocol when we simply raised spatial frequency to 4 cycle deg^{-1}. Spatial frequency thus clearly controls whether L' and M' signals summate positively or negatively in LUM on the orange field at low temporal frequency. We therefore tested whether the other two observers would see the motion reversal *below* 1 cycle deg^{-1}. A frequency-of-seeing curve was measured for left *versus* right motion discrimination at 1 Hz as a function of spatial frequency from 0·31 to 1 cycle deg^{-1}, using the luminance pedestal and M test in spatial–temporal quadrature. The 50%-chance point for the observers C.F.S. and A.C. occurred at 0·53 and 0·83 cycle deg^{-1}, respectively; the motion was reversed *below* this value and not reversed above. (The reversal is not caused by rod intrusion, as shown with the bleaching control.)

We then remeasured the phase shift at various temporal frequencies with a low spatial frequency of 0·31 and 0·71 cycle deg^{-1}. Figure 16 shows that at 0·31 cycle deg^{-1} the phase function now proceeds toward 180 deg at low temporal frequency, just as it did for observer A.S.T. at 1 cycle deg^{-1}. For all observers, the L' and M' signals summate negatively on the orange field at sufficiently low spatial and temporal frequencies. The phase shift is greatest at the lowest spatial frequency.

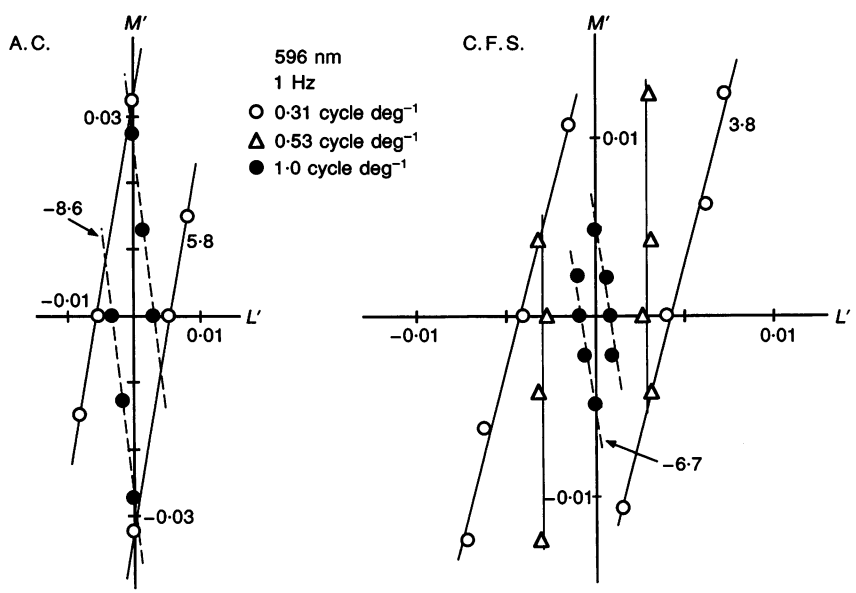

Figure 17. Quadrature motion detection contours on the orange field at 1 Hz and lower spatial frequencies

Contrast thresholds are shown for test patterns having different vector angles in the L', M' co-ordinates, combined in spatial–temporal quadrature with the luminance pedestal. At 0·31 cycle deg^{-1} the contours have a positive slope indicating that L' and M' signals summate negatively in LUM, but at 1 cycle deg^{-1} the slope is negative (positive summation). For C.F.S. at 0·53 cycle deg^{-1} the contour is almost vertical showing *no* effective M' signal in LUM. The slopes are designated beside contours. The average S.E.M. of the data points is 13% for observers A.C. and C.F.S., with a maximal value of 19 and 17%, respectively.

The positive *versus* negative summation of the L' and M' signals in LUM was confirmed by measuring quadrature motion detection contours in the L', M' co-ordinates with 1 Hz stimuli (Stromeyer *et al.* 1995). The counterphase test was combined in spatial–temporal quadrature with the luminance pedestal on the orange field. Pedestal contrast was fixed slightly suprathreshold, and the test contrast was varied to assess the threshold for discriminating the motion direction of the combined pattern. Figure 17 depicts the contrast thresholds of the test pattern *per se*, set at various stimulus vector angles in the L', M' co-ordinates. For observers A.C. and C.F.S., the detection contours at 1 cycle deg^{-1} have a negative slope showing positive summation of L' and M' signals in LUM; but at 0·31 cycle deg^{-1} the slope was positive showing negative summation. At an intermediate value of 0·53 cycle deg^{-1}, the detection contour for observer C.F.S. was almost *vertical*, indicating that for this singular condition there is essentially *no* effective M' signal in LUM. (The vertical slope is consistent with the above frequency-of-seeing curve showing that the motion judgements of the observer for the M test broke down at 0·53 cycle deg^{-1}.) Similar detection contours for observer A.S.T. (not depicted) showed that L' and M' signals summate negatively at 1 cycle deg^{-1} but positively at 4 cycle deg^{-1} (slopes of 6·2 and −7·8, respectively).

Our model can explain the spectrally opponent nature of LUM at low spatial and temporal frequency on the orange field. As spatial frequency is lowered the response of the surround grows relative to the centre. The inhibitory M surround component on the orange field (Fig. 14*A*) then acquires a slightly greater weight than the excitatory M centre component yielding a weak net *inhibitory* M response, whereas the L response remains excitatory. This produces a spectrally opponent response with the L cones strongly dominant. At 0·53 cycle deg^{-1} (Fig. 17, observer C.F.S.) the receptive field centre and surround responses for the M pattern are presumably *equal* but of opposite sign, thus producing complete cancellation for M' stimulation and a vertical detection contour.

The receptive field model was fitted to these new phase results (Fig. 16). The curves for the 0·31 cycle deg^{-1} data are based on the model parameters used for the phase results at 1 cycle deg^{-1} (see legend to Fig. 8), but the relative strength of the surround components have been augmented by 2·1- and 2·3-fold for observers A.C. and C.F.S., respectively. The slopes of the quadrature detection contours (Fig. 17) were determined from the earlier weight fits at 1 cycle deg^{-1} (see legend to Fig. 10) but using these increased surround values. The predicted slopes for the contours were approximately −11 and −7 for A.C. and C.F.S., respectively, at 1 cycle deg^{-1} and 7 and 8, respectively, at 0·31 cycle deg^{-1}, slightly steeper than the measured slopes (Fig. 17). Thus the model with a stronger surround fits the phase and weights on the orange field at the very low spatial frequency.

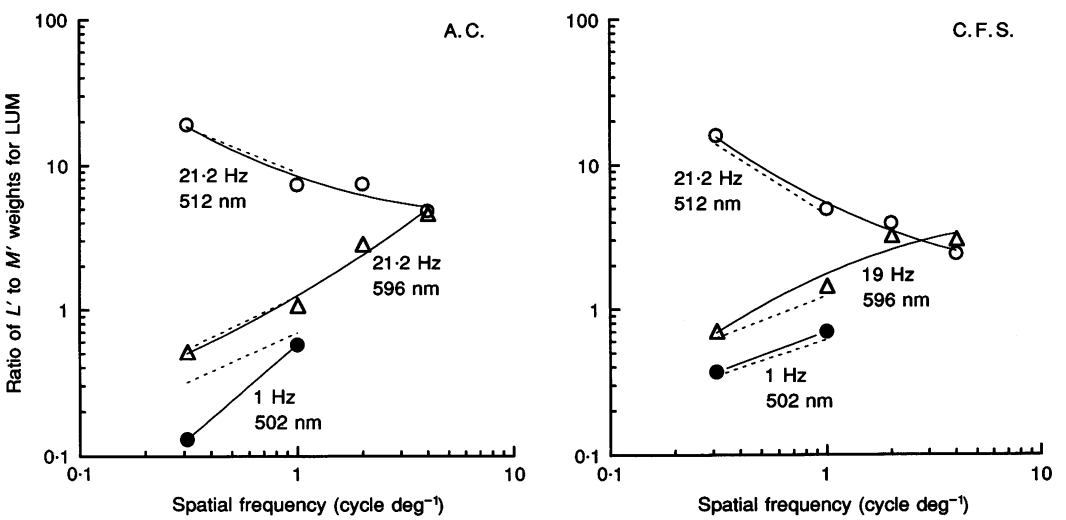

Figure 18. Ratio of L' and M' contrast weights in LUM as a function of spatial frequency at 1 and ~20 Hz on green and orange fields

Weights measured with the quadrature motion protocol. At ~20 Hz the ratio of contrast weights is nearly the same on the green and orange fields for the 4 cycle deg^{-1} patterns which produce little surround response in MC cells. As spatial frequency is lowered the ratio of weights changes in opposite directions on the green and orange fields (○ and △, respectively), demonstrating the presence of the spectrally opponent surround at ~20 Hz. The spectrally opponent surround reverses sign between 1 and ~20 Hz (owing to the large surround delay), as shown by the opposite slopes at 1 and ~20 Hz on the green field (●, ○). A similar effect is observed on the orange field (see text). Dotted lines show fit of model discussed in text. The average S.E.M. of the data points is 17 and 14% for observers A.C. and C.F.S., respectively, with a maximal value of 19 and 19%, respectively.

Measurements on green field at low spatial and temporal frequency. On the orange field, as spatial frequency was lowered the slope of the detection contour (Fig. 17) became steeper and then inverted, owing to the increased effectiveness of the inhibitory M surround. The model predicts the opposite slope change on the green field. As spatial frequency is lowered the slope ought to get flatter, since now the L surround component is inhibitory (Fig. 14*B*) with respect to the L centre, the reverse from the orange adapting condition. The increased L inhibitory surround will thus make the detection contour flatter, or less sensitive along the L contrast axis. The relative L' and M' weights were measured at 1 Hz with the quadrature motion protocol. For observer A.C. the weight ratio, a/b, at 1 *versus* 0·31 cycle deg^{-1} was 0·58 *versus* 0·13 (slope of −0·58 *versus* −0·13), while for observer C.F.S., a/b was 0·70 *versus* 0·37. (These results are also depicted in Fig. 18.) While these slopes become flatter at very low spatial frequency, they do not actually invert and become positive as on the orange field. The LUM mechanism thus does not become spectrally opponent on the green field, but only does so on long-wave adapting fields at sufficiently low spatial and temporal frequency. This latter effect is observed in MC ganglion cells (see Discussion).

Presence of spectrally opponent surround at high temporal frequency

The results above show the increased effect of the surround at low spatial frequency, measured at a low temporal frequency. The final observations reveal the effects of this augmented spectrally opponent surround at a high temporal frequency.

Figure 18 shows the relative L' and M' weights at ~20 Hz as a function of spatial frequency on the green (○) and orange (△) fields. As before, the weights were measured with the quadrature motion protocol, with the L test and the M test combined in optimal temporal phase with the luminance pedestal. (The fields were 1300 td, except for the 512 nm green field, which was 1440 td.) The weight ratio was nearly the same on the green and orange fields at the highest spatial frequency where little surround response is expected. At low spatial frequency the weight ratio was extremely different on the two fields. The M input to LUM is strongly suppressed on the green field and the L input is suppressed on the orange field. A similar suppression was observed by Eisner & MacLeod (1981) with a large uniform flickering spot. Our results show that this suppression only occurs at low spatial frequencies, demonstrating that the surround is necessary for the suppression. The symbol ● shows the weight ratio on the green field reported above at a low temporal frequency of 1 Hz. On the green field, the change in contrast weights with spatial frequency is of opposite slope at 1 Hz (●) *versus* ~21·2 Hz (○), indicating that the spectrally opponent surround has reversed in sign at high temporal frequency owing to the surround delay. The fit of the receptive field model is shown by the end points of the dotted lines connecting results at 0·31 and 1 cycle deg^{-1}. The fit at 1 cycle deg^{-1} is based on parameters used to fit the earlier phase and weight data (Figs 8 and 10). To fit the results at 0·31 cycle deg^{-1} on the orange field, the strength of the surround components was increased 2·1-fold for observer A.C. and 2·3-fold for C.F.S. (as in Fig. 16). On the green field the surrounds were increased 1·3-fold for both observers. On the green field at 21·2 Hz (○), the L' to M' weight ratio rises considerably between 1 and 0·31 cycle deg^{-1} owing to the augmented spectrally opponent surround.

To get the model to predict this latter *large rise* on the green field it was necessary to assume that the centre and surround phasors (Fig. 14) were essentially collinear at 21 Hz, thus producing *maximal cancellation* of the opposite signed, centre and surround M phasors. This required that we increase slightly the surround delay on the green field from the original value of ~7 deg s^{-1} (at 1 cycle deg^{-1}, where the phase shift goes through zero at ~26 Hz) to a slightly larger value of ~8·5 deg s^{-1} (so the phase shift goes through zero at ~21 Hz). This delay difference was confirmed for both observers by measuring the phase shift from 17·7 to 26 Hz. Near 21 Hz the M' signal lagged L' considerably more at 2 *versus* 0·31 cycle deg^{-1}, indicating that the surround delay was slightly greater at the lower spatial frequency. A slightly larger surround delay might be expected as spatial frequency is lowered since more distant regions of the surround may participate. However, we did not see a similar effect on the orange field.

Thus, these results show the clear presence of the spectrally opponent surround at high temporal frequency, and argue for a long surround delay.

DISCUSSION

Adapting colour and the L' *versus* M' phase shift in LUM

The summation of the L' and M' signals in LUM, as reflected in the relative phase shift and contrast weights, is controlled by the mean M/L excitation of the adapting field, with S cones playing little role. To eliminate the phase shift, the adapting field must be carefully selected for each observer within the green–yellow range, 565–570 nm. On such a field there is no phase shift at all spatial and temporal frequencies tested. There thus appears to be a precise chromatic adapting condition for which nominally equiluminant flickering or moving patterns will *not* stimulate LUM owing to the phase shift. On this field the relative L' and M' contrast weights do not vary with temporal frequency.

Errors in measuring the phase shift will occur if the observer's unique L and M stimuli are incorrectly estimated. We obtained particularly large phase shifts on the green field. The apparent phase shift on this field would be augmented if the nominal M test had an inadvertent

negative L component. The model requires that the relative phase shift at intermediate temporal frequencies should not exceed 90 deg if the phase shift asymptotes to 0 deg at both 0 Hz and a higher frequency (such as 20 Hz). Two controls suggest that the large phase shifts (70–80 deg) on the green field are real and do not simply reflect an error in estimating the observer's unique L or M cone axis. A large phase shift at 9 Hz was estimated from motion nulls (Fig. 11) for tests which covered the *full* range of vector angles in the L', M' cone-contrast co-ordinates (rather than being restricted to just the unique L and M axes). A large phase shift was also estimated from motion detection contours (Fig. 6) for drifting gratings covering the full range of angles in the L', M' co-ordinates.

Swanson *et al.* (1988) psychophysically measured the phase shift for minimizing the luminance flicker of alternating red and green lights in a 2 deg test field. On a bright orange adapting background (600 nm), the red light had to be advanced as much as 60 deg at 6 Hz, and the phase shift was zero near 20 Hz. The phase shift at 6 Hz was reduced on a red background and was weakly reversed on a green background. Swanson *et al.* (1988) measured the phase shifts between *lights*, whereas we measured the phase shifts between the L' and M' signals. Swanson (1994) used a model to estimate the L' *versus* M' signal phase shift from the measurements: at 6 Hz on the orange field L' was estimated to lag M' by as much as 110 deg, and at 6 Hz on the green field M' was estimated to lag L' by as much as 30 deg. At high frequency the phase shift reversed. For example, on the orange field at 27 Hz the L' signal was estimated to lead M' by 46 deg. Our results on the orange field (Fig. 8*C*) directly demonstrate this large ~50 deg L' lead at 26–30 Hz; at higher frequencies the lead was reduced. The recordings of MC cells, however, showed rather little relative phase shifts at 20–40 Hz on orange fields (Smith *et al.* 1992).

Several results indicate that the phase shift arises early in the visual system. First, we observed that the phase shift is monocular; changing the chromatic appearance of the adapting field via the other eye had no effect. Second, identical phase shifts were obtained for pure flicker or motion. The extraction of a motion signal must involve a processing delay (a spatial–temporal asymmetry), but this additional delay apparently has no effect on the phase shift, consistent with the view that the phase shift is determined early. Third, very similar phase shifts have been measured in retinal MC cells on an orange field (Smith *et al.* 1992). The MC pathway is strongly involved in detecting motion and flicker. If the phase shift is imposed within the MC retinal cells, then the phase shift must affect all further processing in this pathway. Temporal phase shifts arising in the retinal cells would probably produce spatial phase shifts for uniformly drifting gratings, and indeed we observed that the temporal phase shifts predicted the magnitude of such spatial phase shifts. This is hardly surprising, for the well-known Pulfrich pendulum demonstrates that a change in latency or phase response at an early visual stage causes an apparent spatial displacement of a moving stimulus.

Models of MC retinal ganglion cells

The centre of the MC receptive field sums L' and M' signals, as small heterochromatically flickering lights confined to the centre produce a sharp flicker null, with spectral sensitivity closely matching the V_λ human photopic luminosity function (Lee *et al.* 1988). The luminosity function reflects a simple weighted sum of L and M spectral sensitivities, with an approximately 2-fold greater L weight (Smith & Pokorny, 1975). We measured the L' and M' contrast weights with gratings of 4 cycle deg^{-1} which partially isolate the receptive field centre; the L' *contrast* weight was ~3 times the M' weight on *both* green and orange fields, measured at 4 and ~20 Hz. This constancy of *contrast* weights shows that the L and M cone signals individually adapt on different coloured fields. The V_λ luminosity function does not include provision for cone-selective light adaptation (being based on a constant sum of L and M spectral sensitivities), and thus the V_λ function will probably not describe heterochromatic flicker nulls in the receptive field centre over a wide range of chromatic adaptation of moderate brightness. The large relative phase shifts and changes in contrast weights that we observed at low spatial frequency presumably reflect a centre-surround interaction, since the centre itself simply summates L' and M' signals (Lee *et al.* 1988) and shows little L' *versus* M' phase shift (Smith *et al.* 1992; Kremers *et al.* 1994).

Three controversial features of our model are the modification of the spectral nature of the surround by coloured adapting fields (which is needed to explain the reversed phase shift on green *versus* orange fields), the clear presence of a spectrally opponent surround at high temporal frequencies (20 Hz), and the large surround delay. Our simple model explains both the changes in the relative L' and M' phase shift and contrast weights as a function of temporal frequency. The long surround delay is required to explain the fact that the relative phase shift goes through zero near 20 Hz despite the clear presence of the spectrally opponent surround at 20 Hz. These three features will be discussed in turn.

The first feature is that the spectral nature of the surround is modified by the mean M/L excitation produced by the adapting field. At low temporal frequency, on the orange field the L surround is antagonistic with respect to the centre while the M surround is facilitory; this is reversed on the green field. This change is consistent with the available physiology. Smith *et al.* (1992) observed that *all* MC cells on the orange field show a considerable L' signal phase lag (except for two cells with strong rod input). Both the on-centre and off-centre cells were assumed to have a spectrally opponent surround in which M cones antagonize the centre and L cones facilitate the centre, as in our model. Thus the surrounds of the entire population of MC cells appear to be

chromatically biased on the orange field, as we propose. It is not at all clear what precise mechanism may give rise to the modification of the surround. The anatomical make-up of the surround is poorly understood at present (Croner & Kaplan, 1995), but there may be ample machinery available since the surrounds have input from as many as 1000 cones (Croner & Kaplan, 1995).

Derrington *et al.* (1984) showed that MC cells in the LGN typically gave a spectrally opponent response to a large flickering stimulus (but not to a centre-isolating stimulus). Virtually all the MC cells had chromatically opponent receptive fields, but for many cells the opposite L' and M' weights were quite imbalanced. They used a greenish 'white' adapting field, metameric with 557 nm for the L and M cones. They observed about equal numbers of cells with positive L' weights plus negative M' weights, and vice versa. Our observations (Fig. 4) show that their 'greenish' field induces a substantial phase shift, with the M' signal lagging L'. Our model requires that, on this greenish field, on average, the L surround will be weakly antagonistic with respect to the centre and the M surround will be weakly facilitory. The two classes of cells, with reversed L' and M' weights observed by Derrington *et al.* (1984), may simply reflect the populations of on-centre *versus* off-centre cells (this was not separately reported), for in our model and that of Smith *et al.* (1992) the on-centre and off-centre cells are distinguished by only a sign inversion of all the L and M, centre and surround components.

It would be interesting to know the nature of the chromatic surround on a field of ~567 nm that produces no psychophysical L' *versus* M' phase shift. Two possibilities might arise. First, the individual MC cells may exhibit no L' *versus* M' phase shift; this would imply that the centres and surrounds have matched spectral sensitivity. Second, there may be two populations of on-centre (or off-centre) cells, with surrounds of reversed spectral opponencies (similar to those in Fig 14*A* and *B*), and these may be about *equally represented*; the opposite phase shifts produced by these two populations might then partially cancel for the psychophysical observations which depend upon the *ensemble* of cells.

C. Reid & R. M. Shapley (personal communication) have measured LGN MC cells on such a field, metameric with 567 nm (2000 td) for the L and M cones. They measured the spatio-temporal receptive field structure with cone-isolating dynamic 2-D stimuli (*m*-sequences; method described in Reid & Shapley, 1992). They derived temporal impulse responses for both the L and the M components of centre and surround. (The surround delays for these cells are described below.) The centre summed L' and M' signals, and the surrounds typically did *not* match the spectral sensitivity of the centres. We applied our model to these cells to assess the L' *versus* M' phase shift to large-field luminance flicker: three of the cells showed a substantial relative M' lag whereas three other cells showed the opposite lag. This result appears to support our second hypothesis for why we observed psychophysically little L' *versus* M' phase shift on the 567 nm field, namely that there are two classes of cells producing about opposite phase shifts which cancel for the ensemble.

The second feature of our model is the clear presence of the spectrally opponent surround at high temporal frequencies. This is supported by the large changes in the relative contrast weights that we observed on green *versus* orange fields as spatial frequency was varied. At ~20 Hz the L' signal is ~3 times more effective than M' at 4 cycle deg^{-1} on *both* green and orange fields (Fig. 18), but as spatial frequency is lowered to 0·31 cycle deg^{-1} (thus augmenting the surround response) the L' signal becomes 15–20 times more effective than M' on the green field and the M' signal becomes ~2 times more effective than L' on the orange field. The spectrally opponent surround thus does not simply disappear near 20 Hz, for it is needed to explain the large dependence of the relative L' and M' weights on spatial frequency.

The third feature of our model is the large surround delay, which is unexpected. On the green field the relative phase shift goes through zero at ~26 Hz, leading us to assume a surround delay of ~19 ms. (The delay might be shortened by 2–3 ms by including a possible latency difference between L and M photoreceptors.) The relative phase shift would also go through zero *without* a large surround delay if the centre and surround had matched spectral sensitivity near 20 Hz (Smith *et al.* 1992), but our results on the contrast weights suggest that the centre and surround are not spectrally matched. The long surround delay thus provides a parsimonious explanation of the simultaneous changes in the relative phase shift and relative contrast weights.

Physiology provides fairly extensive estimates of the surround delay for PC cells but there are only sparse estimates for MC cells. For macaque red–green ganglion PC cells, Smith *et al.* (1992) estimated a delay of 3–8 ms (adapting level, 2000 td), based on a receptive field model with an L or M centre and a surround exclusively of the opposite cone type. Using this model and spatially uniform, unique L or M stimuli, Gielen, van Gisbergen & Vendrik (1982) estimated a surround delay of 16 ms at the LGN (adapting level, 250 td).

C. Reid & R. M. Shapley (personal communication) measured the surround delay in LGN MC cells; the delay represented the difference between the temporal impulse responses of centre and surround. Two off-centre cells had a surround delay of ~14 ms, while three on-centre cells had a delay of ~10 ms and one had a delay of ~18 ms. Perhaps the delay would be larger on strongly chromatic fields that induce large L' *versus* M' phase shifts.

Comparison of our model of MC cells with that of Smith *et al.* (1992)

Our model has features in common with that of Smith *et al.* (1992). Both models assume that, for on-centre cells, the centre sums L' and M' signals (and is thus spectrally *non-opponent*) and the surround has an excitatory spectrally *opponent* component, of type +L−M for orange adaptation. (Their model also contains a 'non-opponent' surround component spectrally matched to the centre, which inhibits the centre.) Their model has three independent parameters: the sensitivity ratio, B, of the non-opponent to opponent responses of the cell (this decreases considerably at higher temporal frequency), the phase of the centre response, and the phase of the spectrally opponent surround response. In fitting the phase data, the response of the opponent surround is allowed to have surprising values. For example, at 1·22 Hz the surround response phase may be 90 deg (Table 1 of Smith *et al.* 1992). It is not clear how such a 90 deg phase shift of the *surround response* could arise at very low frequency. A temporal differentiator might introduce a 90 deg phase shift but would be insensitive to slow stimulus variations.

For red and green lights, flickering at the same temporal frequency, the surround spectrally opponent response and the centre non-opponent response may be in approximate quadrature temporal phase with respect to each other assuming that there are no intrinsic, physiological phase shifts. This is a property of the stimulus alone (Lindsey *et al.* 1986). Unless an *intrinsic* phase shift is introduced in the mechanism, the *amplitude* of the summed opponent and non-opponent responses will be *identical* when the red and green flickering lights are combined in relative phase, $\theta = +90$ *versus* -90 deg, and thus will not account for the *asymmetric* amplitude responses observed by Smith *et al.* (1992) at low frequency at these two phases (their Fig. 6).

In our model, in contrast, the relative L and M centre weights and surround weights are fixed by chromatic adaptation. There is also a fixed surround delay, but otherwise there are no free parameters. A main difference between the two models is that the model of Smith *et al.* (1992) ascribes the lack of relative phase shift at ~20 Hz to the decrease in strength of the spectrally opponent surround, whereas we ascribe the absence of phase shift at ~20 Hz to the large surround delay, since the spectrally opponent surround appears to be present at 20 Hz. Either model can explain the absence of relative phase shift at ~20 Hz. Measurements of the relative L' and M' weights of the cells, at ~20 Hz, as a function of spatial frequency could ascertain the spectrally opponent surround.

Further comparisons of MC cells and our measurements of LUM

Measurements of MC retinal ganglion cells reveal additional features agreeing with our measurements. Lee *et al.* (1989) observed that, for a large, 10 Hz flickering spot, the L' and M' signals in the MC cells did not *appear* to summate fully, suggesting a non-linearity. More recently, Lee *et al.* (1993) measured threshold detection contours for MC cells in L', M' co-ordinates; the elliptical shape of these contours shows that the summation is in fact linear when the phase shift is taken into account. Our results (Fig. 6 and Stromeyer *et al.* 1995) show linear summation.

Lee *et al.* (1989) observed that on an adapting field of ~574 nm (metamer for L and M) the L' and M' contrast weights were similar for 10 Hz uniform flicker, but every MC cell showed a significantly greater L' weight at low temporal frequency, similar to our observations that on a yellow 580 nm (Stromeyer *et al.* 1995) or orange field the L' weight increases relative to M' at low temporal frequency.

On the orange field at sufficiently low spatial and temporal frequency we observed that the LUM detection contour has a *positive* slope in the L', M' co-ordinates. Thus for this particular condition LUM is spectrally opponent, responding to the difference of L' and M' signals, with the L' signal clearly dominant. Lee *et al.* (1993) observed a similar effect on an adapting field of ~580 nm (our estimate); for a large flickering spot, the threshold contours of the cell at 10 Hz had a negative slope in the L', M' co-ordinates, but at 2 Hz the slope was positive, showing a spectrally opponent signature with L' dominant. Further physiological measurements could test the unusual features of our model. A reversal of the relative phase shift on orange *versus* green fields would indicate that the spectrally opponent surround is modified by chromatic adaptation. Strong changes in the relative L' and M' weights with spatial frequency at high temporal frequency (20 Hz) would indicate the presence of the spectrally opponent surround at 20 Hz and reinforce the long surround delay.

RG mechanism

We observed no phase shifts (< 3 deg) between the L' and M' signals in RG at 6 Hz on fields ranging from green to red, or at 10 Hz on the red field. Smith *et al.* (1992) concluded that the PC red–green cells had a surround delay of 3–8 ms; cells with L centres and M surrounds and cells with M centres and L surrounds produced *approximately* opposite phase shifts. The psychophysical observations depend on the ensemble of cells. If the phase shifts were exactly opposite in these two cell classes then the psychophysical phase shift might cancel completely. However, the two cell classes were not exactly opposite, consistent with an ~2 ms latency difference between the L and M cones, with the L cones being faster on the orange field (Smith *et al.* 1992). However, if we suppose that on the deep-red field this latency difference increased to 7 ms, calculations show that such a latency difference would produce an ~15 deg shift in the symmetry axis of the phase template at 6 Hz (a latency difference of 5 ms would produce a similar effect at 10 Hz). This is based on a model in which the centre has L cones and the surround M cones or vice versa (Smith *et al.* 1992; Reid & Shapley, 1992) with equal contrast weights. A similar size effect is also expected for a mixed (L + M) antagonistic cone surround, where the weight of the surround cone of the same type as the centre is, for example, two-thirds of the

centre weight. The two opposite sets of red–green cells would not nullify the phase shift owing to such cone latency differences.

We are surprised that the sensitive template method does not reveal a cone latency effect. The large differences in the phase shifts in LUM on the orange *versus* red field suggest the presence of some photoreceptor latency difference. However, recordings of S cone centre PC ganglion cells on an orange field revealed virtually *no* phase shift between the L' and M' surround signals up to 40 Hz, suggesting little differential latency of L and M cones (Smith *et al.* 1992). However, latency differences dependent on light adaptation are clearly apparent in psychophysical studies of the S cone pathways. These latency differences may arise in the S cones, since the dependence of the latency difference on light adaptation is similar whether the S' signal feeds luminance or chromatic pathways (Stromeyer *et al.* 1991).

Perceptual consequences of the phase shifts

The lack of L' *versus* M' phase shifts in RG has consequences for everyday vision. A rapidly moving luminance grating should continue to appear as a pattern of light and dark stripes without colour, since RG has little phase shift and has equal and opposite L' and M' weights, thus poorly responding to moving pure luminance patterns. We in fact observed no spatial colour variations in our moving luminance gratings. More complex luminance patterns like the Benham top will evoke colour sensations, but these colours depend upon complex interactions not necessarily in the retina.

The large L' *versus* M' phase shift in LUM will cause a nominal pure coloured moving grating to directly stimulate LUM. On coloured fields that deviate strongly from green–yellow, there may be no motion-blind directions for LUM within the L',M' co-ordinates. However, these moving patterns detected via LUM will continue to appear achromatic, since LUM does not evoke colour sensations. Our nominal equiluminant moving patterns generally appear as rapid colourless streaming near threshold when detected by LUM. The phase shifts would provide distinct advantages in allowing the luminance pathways to respond well to coloured patterns, for chromatic mechanisms acting alone yield poor speed discrimination at low contrast (Cropper, 1994) and are particularly poor at direction discrimination outside the fovea (Gegenfurtner & Hawken, 1995).

Anstis, S. M. & Cavanagh, P. (1983). A minimum motion technique for judging equiluminance. In *Colour Vision: Physiology and Psychophysics*, ed Mollon, J. D. & Sharpe, L. T., pp. 155–166. Academic Press, New York.

Benardete, E. A., Kaplan, E. & Knight, B. W. (1992). Contrast gain control in the primate retina: P-cells are not X-like, some M-cells are. *Visual Neuroscience* **8**, 483–486.

Cavanagh, P. & Anstis, S. (1991). The contribution of color to motion in normal and color-deficient observers. *Vision Research* **31**, 2109–2148.

Chaparro, A., Stromeyer, C. F. III, Chen, G. & Kronauer, R. E. (1995). Human cones appear to adapt at low light levels: measurements on the red–green detection mechanism. *Vision Research* **35**, 3103–3118.

Croner, L. J. & Kaplan, E. (1995). Receptive fields of P and M ganglion cells across the primate retina. *Vision Research* **35**, 7–24.

Cropper, S. J. (1994). Velocity discrimination in chromatic gratings and beats. *Vision Research* **34**, 41–48.

Cropper, S. J. & Derrington, A. M. (1994). Motion of chromatic stimuli: first-order or second-order? *Vision Research* **34**, 49–58.

Derrington, A. M., Krauskopf, J. & Lennie, P. (1984). Chromatic mechanisms in lateral geniculate nucleus of macaque. *Journal of Physiology* **357**, 241–265.

Derrington, A. M. & Lennie, P. (1984). Spatial and temporal contrast sensitivities of neurones in lateral geniculate nucleus of macaque. *Journal of Physiology* **357**, 219–240.

Donner, K., Koskelainen, A., Djuspsund, K. & Hemilä, S. (1995). Changes in retinal time scale under background light: observations on rod and ganglion cells in frog retina. *Vision Research* **35**, 2255–2266.

Eisner, A. & MacLeod, D. I. A. (1981). Flicker photometric study of chromatic adaptation: selective suppression of cone inputs by colored backgrounds. *Journal of the Optical Society of America* **71**, 705–718.

Enroth-Cugell, C. & Robson, J. G. (1966). The contrast sensitivity of retinal ganglion cells of the cat. *Journal of Physiology* **187**, 517–552.

Enroth-Cugell, C., Robson, J. G., Schweitzer-Tong, D. E. & Watson, A. B. (1983). Spatio-temporal interactions in cat retinal ganglion cells showing linear spatial summation. *Journal of Physiology* **341**, 279–307.

Gegenfurtner, K. R. & Hawken, M. J. (1995). Temporal and chromatic properties of motion mechanisms. *Vision Research* **35**, 1547–1563.

Gielen, C. C. A. M., van Gisbergen, J. A. M. & Vendrik, A. J. H. (1982). Reconstruction of cone-system contributions to the responses of colour-opponent neurones in monkey lateral geniculate nucleus. *Biological Cybernetics* **44**, 211–221.

Kremers, J., Yeh, T. & Lee, B. B. (1994). The response of macaque ganglion cells and human observers to heterochromatically modulated lights: the effect of stimulus size. *Vision Research* **34**, 217–221.

Lee, B. B., Martin, P. R. & Valberg, A. (1988). The physiological basis of heterochromatic flicker photometry demonstrated in ganglion cells of the macaque retina. *Journal of Physiology* **404**, 323–347.

Lee, B. B., Martin, P. R. & Valberg, A. (1989). Sensitivity of macaque retinal ganglion cells to chromatic and luminance flicker. *Journal of Physiology* **414**, 223–243.

Lee, B. B., Martin, P. R., Valberg, A. & Kremers, J. (1993). Physiological mechanisms underlying psychophysical sensitivity to combined luminance and chromatic modulation. *Journal of the Optical Society of America* **A10**, 1403–1412.

Lee, B. B., Pokorny, J., Smith, V. C. & Kremers, J. (1994). Responses to pulses and sinusoids in macaque ganglion cells. *Vision Research* **34**, 3081–3096.

Lee, J. & Stromeyer, C. F. III (1989). Contribution of human short-wave cones to luminance and motion detection. *Journal of Physiology* **413**, 563–593.

Lennie, P., Pokorny, J. & Smith, V. C. (1993). Luminance. *Journal of the Optical Society of America* **A10**, 1283–1293.

Levinson, E. & Sekuler, R. (1975). The independence of channels in human vision selective for direction of movement. *Journal of Physiology* **250**, 347–366.

Lindsey, D. T., Pokorny, J. & Smith, V. C. (1986). Phase-dependent sensitivity of heterochromatic flicker. *Journal of the Optical Society of America* **A3**, 921–927.

Merigan, W. H. (1989). Chromatic and achromatic vision of macaques: role of the P pathway. *Journal of Neuroscience* **9**, 776–783.

Merigan, W. H., Byrne, C. E. & Maunsell, J. H. R. (1991). Does primate motion perception depend on the magnocellular pathway? *Journal of Neuroscience* **11**, 3422–3429.

Poirson, A. B., Wandell, B. A., Varner, D. & Brainard, D. H. (1990). Surface characterizations of color thresholds. *Journal of the Optical Society of America* **A7**, 783–789.

Reid, R. C. & Shapley, R. M. (1992). Spatial structure of cone inputs to receptive fields in primate lateral geniculate nucleus. *Nature* **356**, 716–718.

Rushton, W. A. H. & Powell, D. S. (1972). The rhodopsin content and the visual threshold of human rods. *Vision Research* **12**, 1073–1081.

Schiller, P. H., Logothetis, N. K. & Charles, E. R. (1990). Role of the color-opponent and broad-band channels in vision. *Visual Neuroscience* **5**, 321–346.

Smith, V. C., Lee, B. B., Pokorny, J., Martin, P. R. & Valberg, A. (1992). Responses of macaque ganglion cells to the relative phase of heterochromatically modulated lights. *Journal of Physiology* **458**, 191–221.

Smith, V. C. & Pokorny, J. (1975). Spectral sensitivity of the foveal cone photopigments between 400 and 500 nm. *Vision Research* **15**, 161–171.

Stockman, A., MacLeod, D. I. A. & Vivien, J. A. (1993). Isolation of the middle- and long-wavelength-sensitive cones in normal trichromats. *Journal of the Optical Society of America* **A10**, 2471–2490.

Stockman, A. & Plummer, D. J. (1994). The luminance channel can be opponent? *Investigative Ophthalmology and Visual Science* **35**, 1572.

Stromeyer, C. F. III, Cole, G. R. & Kronauer, R. E. (1987). Chromatic suppression of cone inputs to the luminance flicker mechanism. *Vision Research* **27**, 1113–1137.

Stromeyer, C. F. III, Eskew, R. T. Jr, Kronauer, R. E. & Spillmann, L. (1991). Temporal phase response of the short-wave cone signal for color and luminance. *Vision Research* **31**, 787–803.

Stromeyer, C. F. III, Kronauer, R. E., Madsen, J. C. & Klein, S. A. (1984). Opponent-movement mechanisms in human vision. *Journal of the Optical Society of America* **A1**, 876–884.

Stromeyer, C. F. III, Kronauer, R. E., Ryu, A., Chaparro, A. & Eskew, R. T. Jr (1995). Contributions of human long-wave and middle-wave cones to motion detection. *Journal of Physiology* **485**, 221–243.

Swanson, W. H. (1994). Time, color, and phase. In *Visual Science and Engineering: Models and Applications*, ed. Kelly, D. H., pp. 191–225. Marcel Dekker, New York.

Swanson, W. H., Pokorny, J. & Smith, V. C. (1988). Effects of chromatic adaptation on phase-dependent sensitivity to heterochromatic flicker. *Journal of the Optical Society of America* **A5**, 1976–1982.

Acknowledgements

This research was supported by NIH grants EY11246, EY01808 and the Milton Fund.

Author's email address

C. F. Stromeyer: charles@stokes.harvard.edu

Received 19 June 1996; accepted 13 November 1996.